B4: Subatomic Physics

Toby Adkins

June 19, 2017

Contents

1. *Scattering and Resonances*

In this chapter, we examine some of the basic concepts underlying the study of subatomic scales, including:

- Scattering Theory
- Partial Wave Analysis
- Feynman Diagrams
- Resonances

This chapter will serve as an introduction to the study of Subatomic Physics, and as such, we will not be dealing with some of the well-known subatomic particles, such as quarks. Instead, we shall examine some of the methods that we can use to determine the workings of the universe on subatomic scales. Though technically not on the syllabus, this author has chosen to include partial wave analysis in this, as it is a useful tool that students should be familiar with at a cursory level.

Note that throughout this text, we will be adopting the metric

$$\eta_{\mu\nu} = \text{diag}(-1, 1, 1, 1)$$

1.1 Scattering Theory

The main method used to determine the composition of some structure is to accelerate a particle towards it, and monitor the trajectory of said particle as it passes by - or through - said structure. Provided that the target structure is sufficiently thin (in comparison to the accelerated particles) such that the flux is approximately constant within the target, the number of particles per unit solid angle $n(\theta, \phi)$ (per unit time) seen at the detector is proportional to the incoming flux j_A. The constant of proportionality is the *scattering cross section*, defined as

$$\sigma = \int d\Omega \, \frac{d\sigma}{d\Omega}, \quad \frac{d\sigma}{d\Omega} = \frac{\text{Particles per solid angle}}{\text{Incoming flux}} = \frac{n}{j_A} \tag{1.1}$$

The scattering cross section represents an 'effective area' presented by the target for the scattering process. We usually work in terms of the differential cross section $d\sigma/d\Omega$ (cross section per unit solid angle of the scattered particle), as we can then integrate over the desired range of angles.

1.1.1 Classical Scattering

Let us initially examine the case where all objects involved in the process are treated as simple classical objects in order to get a feel for the sort of calculations that are required. For some central potential $V(r)$, the angle of scattering is determined by the *impact parameter* b. The number of particles scattered per unit time in the range $[\theta, \theta + d\theta]$ is equal to the number of incident particles per unit time in the range $[b, b + db]$. Therefore, for an incident flux j_A, the number of particles scattered into the solid angle $d\Omega = \sin\theta d\theta d\phi$ per unit time is given by

$$n d\Omega = n \sin\theta d\theta d\phi = j_A b db d\phi \tag{1.2}$$

meaning that the differential cross-section for classical scattering is given by

$$\boxed{\frac{d\sigma}{d\Omega} = \frac{b}{\sin\theta}\left|\frac{db}{d\theta}\right|} \tag{1.3}$$

Hard Sphere Scattering

Consider the case of a projectile being scattered off a hard sphere potential of the form

$$V(r) = \begin{cases} 0 & \text{for } r > R \\ \infty & \text{for } r \leq R \end{cases} \tag{1.4}$$

From figure 1.1, it is clear that

$$b(\theta) = R\sin\alpha = R\sin\left(\frac{\pi - \theta}{2}\right) = -R\cos\theta/2 \tag{1.5}$$

from which, using (1.3), it follows quickly that

$$\frac{d\sigma}{d\Omega} = \frac{R^2}{4} \tag{1.6}$$

This result is what we expect; the total scattering cross section is simply πR^2, the projected area of the sphere as seen from the source.

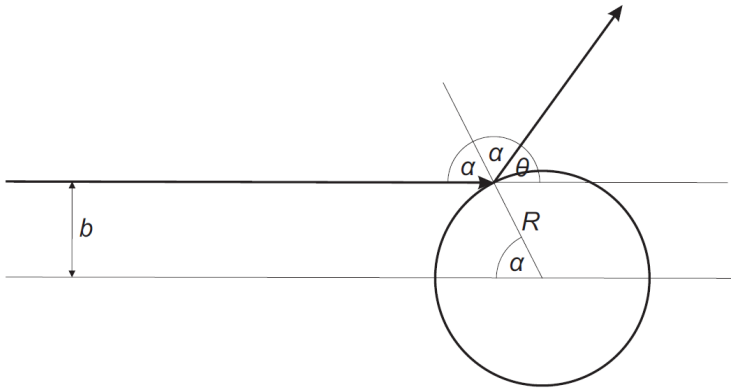

Figure 1.1: Scattering from a hard sphere potential of radius R

Classical Rutherford Scattering

Rutherford scattering is the scattering of a particle of charge $Z_1 e$ from the Coulomb potential of a nucleus with a charge $Z_2 e$, vis.:

$$V(r) = \frac{Z_1 Z_2 e^2}{4\pi\epsilon_0 r} \tag{1.7}$$

The conservation of angular momentum gives

$$mr^2\dot{\beta} = mv_0 b \quad \longrightarrow \quad \frac{d\beta}{dt} = \frac{v_0 b}{r^2} \tag{1.8}$$

where v_0 is the initial velocity, while r and β are as defined in figure 1.2. The change in momentum of the particle is then

$$\Delta p = 2mv_0 \sin\left(\frac{\theta}{2}\right) = -\int_{-\infty}^{\infty} dt\, \cos\beta\, \nabla U = \frac{Z_1 Z_2 e^2}{2\pi\epsilon_0 v_0 b}\cos\left(\frac{\theta}{2}\right) \tag{1.9}$$

such that the impact parameter is given by

$$b = \frac{Z_1 Z_2 e^2}{4\pi\epsilon_0 m v_0^2}\cot\left(\frac{\theta}{2}\right) = \frac{d}{2}\cot\left(\frac{\theta}{2}\right) \tag{1.10}$$

where we have define the distance of closest approach for $b = 0$ (balance between kinetic energy and that due to the Coulomb repulsion).

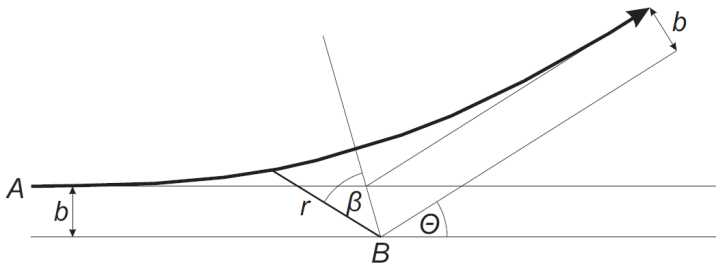

Figure 1.2: Rutherford scattering from a Coulomb potential

From (1.3), it follows that the differential scattering cross section is given by

$$\boxed{\frac{d\sigma}{d\Omega} = \frac{d^2}{16}\frac{1}{\sin^4(\theta/2)}} \tag{1.11}$$

This is the famous *Rutherford scattering formula*. This agrees very well with experiment until the energy of the incident (alpha) particles reaches $\backsim$ 27.5 MeV, after which the scattered intensity drops off sharply, suggesting that there is more to the nucleus than we first expect. Note that the cross-section diverges for $\theta \to 0$; this is because the cross-section is only meaningful down to some finite minimum scattering angle θ_{min} corresponding to a maximum impact parameter.

1.1.2 Quantum Mechanical Scattering

We shall restrict ourselves to non-relativistic considerations. As such, we need to solve the following form of the Time-Independent Schródinger equation:

$$(H_0 - E)\,|\psi\rangle = -V\,|\psi\rangle \tag{1.12}$$

where H_0 is the Hamiltonian in the case that the scattering potential $V = 0$, and E is the corresponding energy. Suppose that

$$H_0\,|\phi\rangle = E\,|\phi\rangle \tag{1.13}$$

Then, the solution to (1.12) can be written as

$$|\psi\rangle = |\phi\rangle + \frac{V}{E - H_0 \pm i\varepsilon}\,|\psi\rangle \tag{1.14}$$

where we have introduced a small parameter $\varepsilon \to 0$ in order to avoid the divergence associated with the singular operator $1/(E - H_0)$. This is known as the *Lippmann-Schwinger equation* for non-relativistic quantum mechanical scattering. We shall now solve this in the position representation. Bra'ing throughout by $\langle \mathbf{x}|$, it follows that

$$\begin{aligned}\langle \mathbf{x}|\psi\rangle &= \langle \mathbf{x}|\phi\rangle + \int d^3\mathbf{x}'\ \langle \mathbf{x}|\,\frac{1}{E - H_0 \pm i\varepsilon}\,\big|\mathbf{x}'\big\rangle\,\big\langle \mathbf{x}'\big|\,V\,|\psi\rangle \\ &= \langle \mathbf{x}|\phi\rangle + \int d^3\mathbf{x}'\ \langle \mathbf{x}|\,\frac{1}{E - H_0 \pm i\varepsilon}\,\big|\mathbf{x}'\big\rangle\,V(\mathbf{x}')\,\big\langle \mathbf{x}'\big|\psi\big\rangle\end{aligned} \tag{1.15}$$

where we have inserted another identity operator to arrive at the last line. We now need to find an explicit form of the Green's function:

$$G_\pm(\mathbf{x}, \mathbf{x}') = \langle \mathbf{x}|\,\frac{1}{E - H_0 \pm i\varepsilon}\,\big|\mathbf{x}'\big\rangle \tag{1.16}$$

Recalling that

$$\langle \mathbf{x}|\mathbf{p}\rangle = \frac{1}{(2\pi\hbar)^{3/2}}\,e^{i\mathbf{x}\cdot\mathbf{p}/\hbar} \tag{1.17}$$

(1.16) can be written in the momentum representation as

$$\begin{aligned}G_\pm(\mathbf{x}, \mathbf{x}') &= \int d^3\mathbf{p}\ \langle \mathbf{x}|\mathbf{p}\rangle\,\frac{1}{E - p^2/2m \pm i\varepsilon}\,\big\langle \mathbf{p}\big|\mathbf{x}'\big\rangle \\ &= -\frac{2m}{(2\pi\hbar)^3}\int d^3\mathbf{p}\,e^{i(\mathbf{x}-\mathbf{x}')\cdot\mathbf{p}/\hbar}\,\frac{1}{p^2 - 2mE \pm i\varepsilon}\end{aligned} \tag{1.18}$$

Note that as we aim to take $\varepsilon \to 0$, we are going to ignore any numerical factors that it collects. Let $r = |\mathbf{r}| = |\mathbf{x} - \mathbf{x}'|$, and convert to spherical polars in momentum space:

$$\begin{aligned} G_{\pm}(\mathbf{x}, \mathbf{x}') &= -\frac{2m}{(2\pi\hbar)^3} \int_0^\infty dp\, p^2 \int_0^{2\pi} d\phi \int_{-1}^{1} d(\cos\theta)\, e^{ipr\cos\theta/\hbar} \frac{1}{p^2 - 2mE \pm i\varepsilon} \\ &= \frac{1}{(2\pi\hbar)^3} \frac{2mi}{r} \int_{-\infty}^{\infty} dp\, \frac{p e^{ipr/\hbar}}{(p - \hbar k \mp i\varepsilon)(p + \hbar k \pm i\varepsilon)} \end{aligned} \tag{1.19}$$

where we have introduced $E = \hbar k$ (plane wave solutions, valid for a beam that is wide in comparison to k^{-1}, and ignored terms of $\mathcal{O}(\varepsilon^2)$. We now have to invoke some maths from complex analysis. Namely, *Cauchy's Residue Theorem* states that for a complex valued function $f(z)$ with poles at $z = z_n$, the value its integral around some closed contour Γ is given by

$$\oint_\Gamma dz\, f(z) = 2\pi i \sum_n \mathrm{Res}(f(z = z_n)) \tag{1.20}$$

where $\mathrm{Res}(f(z = z_n))$ is a residue contained within the contour Γ. We choose to evaluate our contour in the upper half-plane, such that the enclosed pole is $p = \hbar k + i\varepsilon$. It follows that

$$G_{\pm}(\mathbf{x}, \mathbf{x}') = -\frac{2m}{\hbar^2} \frac{e^{\pm ik|\mathbf{x}-\mathbf{x}'|}}{4\pi|\mathbf{x} - \mathbf{x}'|} \tag{1.21}$$

such that the Lippmann-Schwinger equation becomes

$$\boxed{\langle \mathbf{x}|\psi\rangle = \langle \mathbf{x}|\phi\rangle - \frac{1}{4\pi}\frac{2m}{\hbar^2} \int d^3\mathbf{x}'\, \frac{e^{ik|\mathbf{x}-\mathbf{x}'|}}{|\mathbf{x} - \mathbf{x}'|} V(\mathbf{x}') \langle \mathbf{x}'|\psi\rangle} \tag{1.22}$$

where we have chosen the positive Green's function solution, corresponding to plane waves propagating outwards from the scattering centre. Assuming that the potential is sufficiently localised ($|\mathbf{x}|V \to 0$ as $|\mathbf{x}| \to \infty$), the detector will be sufficiently far from the scattering centre that we can write that $|\mathbf{x}| \gg |\mathbf{x}'|$, and expand the exponential factor as

$$|\mathbf{x} - \mathbf{x}'| = |\mathbf{x}| \left(1 + \frac{|\mathbf{x}'|^2}{|\mathbf{x}|^2} - 2\frac{\mathbf{x}\cdot\mathbf{x}'}{|\mathbf{x}|^2}\right)^{1/2} \approx |\mathbf{x}| \left(1 - \frac{\mathbf{x}\cdot\mathbf{x}'}{|\mathbf{x}|} + \dots\right) \tag{1.23}$$

To first order, the $|\mathbf{x} - \mathbf{x}'|$ in the denominator of (1.22) can be replaced with $|\mathbf{x}|$, while for the phase factor, we must use (1.23), yielding

$$\langle \mathbf{x}|\psi\rangle = \langle \mathbf{x}|\phi\rangle - \frac{1}{4\pi}\frac{2m}{\hbar^2}\frac{e^{ikr}}{r} \int d^3\mathbf{x}'\, e^{-i\mathbf{k}'\cdot\mathbf{x}'} V(\mathbf{x}') \langle \mathbf{x}'|\psi\rangle \tag{1.24}$$

where now $r = |\mathbf{x}|$. However, this remains an integral equation for $\langle \mathbf{x}|\psi\rangle$, meaning that we need some sort of simplification in order for it to be useful. Assuming that the incoming particles can be represented as plane waves of the form

$$\langle \mathbf{x}|\phi\rangle = \frac{1}{(2\pi)^{3/2}} e^{i\mathbf{k}\cdot\mathbf{x}} \tag{1.25}$$

The Lippmann-Schwinger equation becomes

$$\langle \mathbf{x}|\psi\rangle = \frac{1}{(2\pi)^{3/2}} \left[e^{i\mathbf{k}\cdot\mathbf{x}} + \frac{e^{ikr}}{r} f(\mathbf{k}', \mathbf{k})\right] \tag{1.26}$$

Our solution is thus the sum of an incoming plane wave, and an outgoing spherical wave with *scattering amplitude* given by

$$\boxed{f(\mathbf{k}, \mathbf{k}') = -\frac{1}{4\pi}(2\pi)^3 \frac{2m}{\hbar^2} \langle \mathbf{k}'| V |\psi\rangle} \tag{1.27}$$

We shall ignore the interference between the original plane wave and the scattered wave, which is equivalent to assuming that the incoming beam of particles is only approximately a plane wave over a region of dimension much smaller than the value of r. We then find that the partial cross section $d\sigma$ is given by

$$d\sigma = r^2 \frac{|j_{\text{scattered}}|}{|j_{\text{incident}}|} d\Omega = |f(\mathbf{k}, \mathbf{k}')|^2 d\Omega \tag{1.28}$$

such that

$$\boxed{\frac{d\sigma}{d\Omega} = |f(\mathbf{k}, \mathbf{k}')|^2} \tag{1.29}$$

This is a neat result; the differential cross section is simply the mod-squared value of the scattering amplitude.

The Born Approximation

Under the Born approximation, we assume that the perturbation due to the scattering is small, such that to first order, $|\psi\rangle \approx |\phi\rangle$. This means that we can write (1.24) as

$$\langle \mathbf{x}|\psi\rangle^{(1)} = \langle \mathbf{x}|\phi\rangle - \frac{1}{4\pi}\frac{2m}{\hbar^2}\frac{e^{ikr}}{r}\int d^3\mathbf{x}'\, e^{-i\mathbf{k}'\cdot\mathbf{x}'} V(\mathbf{x}') \langle \mathbf{x}'|\phi\rangle \tag{1.30}$$

and the scattering amplitude becomes

$$\boxed{f^{(1)}(\mathbf{k}, \mathbf{k}') = -\frac{1}{4\pi}(2\pi)^3 \frac{2m}{\hbar^2} \langle \mathbf{k}'| V |\mathbf{k}\rangle = -\frac{1}{4\pi}\frac{2m}{\hbar^2}\int d^3\mathbf{x}'\, e^{i(\mathbf{k}-\mathbf{k}')\cdot\mathbf{x}'} V(\mathbf{x}')} \tag{1.31}$$

which is simply the Fourier transform of the potential. By scattering particles from targets, we can thus measured $d\sigma/d\Omega$, and from this infer a form of $V(\mathbf{x})$.

Under what conditions is it valid to make this approximation? We require that the difference between the solution to the Lippmann-Schwinger equation and the incoming plane wave is small:

$$\left|\langle \mathbf{x}|\psi\rangle^{(1)} - \langle \mathbf{x}|\phi\rangle\right| \ll \left|\langle \mathbf{x}|\psi\rangle^{(1)}\right| \tag{1.32}$$

This condition essentially corresponds to the scattering potential being small enough that it does not have a corresponding bound state. We can approximate this by again using $|\psi\rangle \approx |\phi\rangle$, evaluating at $\mathbf{x}' = 0$, and assuming a box-potential of the form

$$V(r) = \begin{cases} -V_0 & \text{for } |\mathbf{x}| \leq a \\ 0 & \text{for } |\mathbf{x}| > a \end{cases} \tag{1.33}$$

This yields the conditions

$$|V_0| \ll \frac{\hbar^2 k}{ma} \text{ for } ka \gg 1, \quad \text{and} \quad |V_0| \ll \frac{\hbar^2}{ma^2} \text{ for } ka \lesssim 1 \tag{1.34}$$

Form Factors

In light of what we have learnt from a quantum mechanical treatment of scattering, let us revisit the case of scattering from a Coulomb like potential. Suppose that a particle of charge $Z_1 e$ is incident on a nucleus of atomic number Z_2 with some spherically symmetric local charge density $\rho(r)$ located at the origin. The potential at some point $\mathbf{x}'$ is then given by

$$V(\mathbf{x}') = \frac{Z_1 e^2}{4\pi\epsilon_0}\int d^3\mathbf{x}''\, \frac{\rho(\mathbf{x}'')}{|\mathbf{x}' - \mathbf{x}''|} = Z_1 \hbar c \alpha_{EM} \int d^3\mathbf{x}''\, \frac{\rho(\mathbf{x}'')}{|\mathbf{x}' - \mathbf{x}''|} \tag{1.35}$$

where we have introduced the electromagnetic fine structure constant $\alpha_{\text{EM}} = \hbar/(m_e a_0 c)$. Substituting this into the scattering amplitude relation (1.31), we have that

$$f^{(1)}(\Delta\mathbf{k}) = AZ_1\hbar c\alpha_{\text{EM}} \int d^3\mathbf{x}' \int d^3\mathbf{x}'' \, e^{i(\Delta\mathbf{k})\cdot\mathbf{x}'} \, \frac{\rho(\mathbf{x}'')}{|\mathbf{x}' - \mathbf{x}''|} \tag{1.36}$$

where we have introduced $A = -m/(2\pi\hbar^2)$. Note that sometimes the momemtum transfer $\Delta\mathbf{k} = \mathbf{k} - \mathbf{k}'$ is written as $\mathbf{q}$, notation that we shall now adopt. Again defining $\mathbf{r} = \mathbf{x} - \mathbf{x}'$, it follows that'

$$f(\mathbf{q}) = \underbrace{\frac{1}{Z}\int d^3\mathbf{x}\, \rho(\mathbf{x}) e^{i\mathbf{q}\cdot\mathbf{x}}}_{\text{Form Factor}} \times \underbrace{AZ_1Z_2\hbar c\alpha_{\text{EM}} \int d^3\mathbf{r}\, \frac{e^{-i\mathbf{q}\cdot\mathbf{r}}}{r}}_{\text{Rutherford scattering amplitude}} \tag{1.37}$$

The total scattering amplitude is thus the product of the Fourier transforms of two terms. The second is easily recognisable as the Rutherford scattering amplitude from a charge distribution $\rho(\mathbf{x}) = Z_2\, \delta^3(\mathbf{x})$. This tells us nothing about the structure of the target nucleus; all the interesting information is contained in the first term:

$$\boxed{F_{\text{nucl}}(\mathbf{q}) = \frac{1}{Z}\int d^3\mathbf{x}\, \rho(\mathbf{x}) e^{i\mathbf{q}\cdot\mathbf{x}}} \tag{1.38}$$

This means that the potential of the nucleus is thus a convolution of a Rutherford like object with a more complicated charge distribution $\rho(\mathbf{x})$. From (1.29), we can thus write that

$$\frac{d\sigma}{d\Omega} = |F_{\text{nucl}}(\mathbf{q})|^2 \left(\frac{d\sigma}{d\Omega}\right)_{\text{Rutherford}} \tag{1.39}$$

By examining the form factor for particles scattered with various values of momentum transfer $\mathbf{q}$, we can infer information about $\rho(\mathbf{x})$ and hence the form of the nuclear potential $V(\mathbf{x})$. Some example form factors are shown in figure 1.3.

The Yukawa Potential

Recall the Klein-Gordan equation that was introduced in B2: Special Relativity and Symmetry:

$$(-\partial_\rho\partial^\rho + \mu^2)\phi = 0, \quad \mu = \frac{mc}{\hbar} \tag{1.40}$$

where ϕ is some non-relativistic field. Assuming that the field is spherically symmetric $\phi = \phi(r,t)$, and that we are in the low frequency limit, such that time derivatives are of much smaller magnitude than spatial derivatives. Then, the Klein-Gordan equation becomes

$$(\nabla^2 - \mu^2)\phi = 0 \quad \longrightarrow \quad \frac{1}{r}\frac{\partial^2}{\partial r^2}(r\phi) = \mu^2\phi \tag{1.41}$$

This has general solution

$$\phi = \frac{c_1}{r}e^{-\mu r} + \frac{c_2}{r}e^{\mu r} \tag{1.42}$$

for constants c_1 and c_2. For properly bounded solutions, we set $c_2 = 0$. This solution is closely related to the *Yukawa potential*

$$\boxed{V(r) = \frac{g^2}{4\pi}\frac{e^{-\mu r}}{r}} \tag{1.43}$$

where the constant g parametrises the strength of the interaction. The scattering amplitude in this case is then given by (1.31)

$$f^{(1)}(\mathbf{q}) = -\frac{2m}{\hbar^2}\frac{1}{q}\int_0^\infty dr\, rV(r)\sin(qr) = -\frac{g^2}{4\pi}\frac{2m}{\hbar^2}\frac{1}{q^2+\mu^2} \tag{1.44}$$

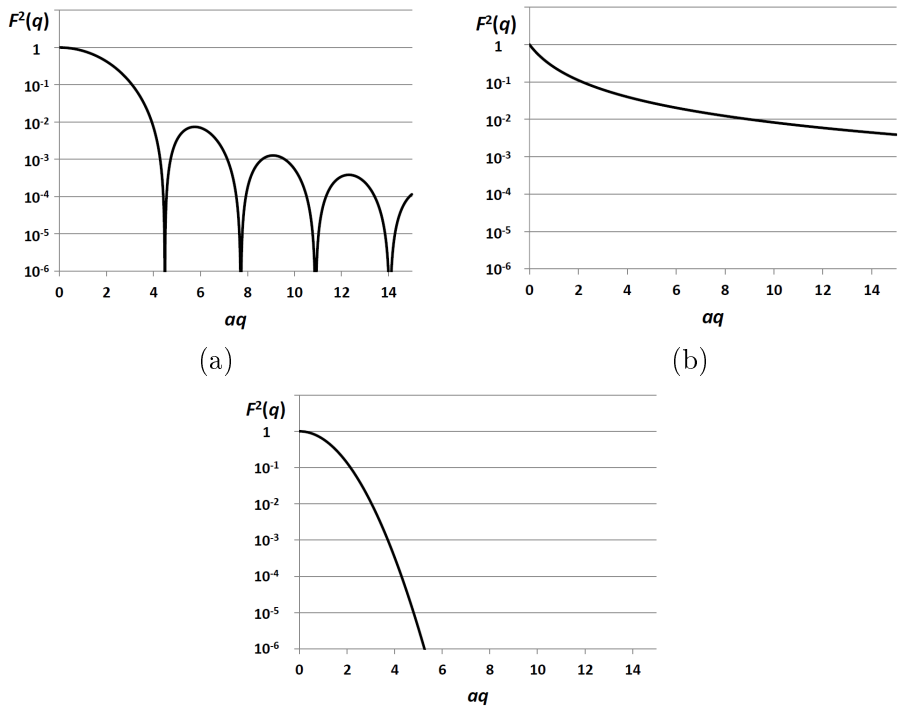

Figure 1.3: Nuclear form factors for (a) Uniformly charged sphere (b) Exponential distribution (c) Gaussian distribution

where the first expression follows from transforming to spherical polars. The associated differential cross section is then given by

$$\frac{d\sigma}{d\Omega}^{(1)} = \frac{g^4}{(4\pi)^2}\left(\frac{2m}{\hbar^2}\right)^2 \frac{1}{[2k^2(1-\cos\theta)+\mu^2]^2} \tag{1.45}$$

where we have made use of the fact that $q = |\mathbf{q}| = 2k\sin\theta/2$. It is clear that this re-obtains the classical Rutherford result for $\mu \to 0$.

Obviously, μ^{-1} represents some lengthscale of the potential. With this, we can associate a mass $m = \hbar\mu/c$, which leads to the concept of a *virtual exchange particle* that is created, and then absorbed (meaning that these cannot be directly observed), in an interaction between two particles that involves a force. As these do not obey the usual energy-momentum invariant $\mathsf{P}\cdot\mathsf{P} \neq -(E/c)^2 + p^2$, they are often known as *off mass-shell* particles. We can associate with these a *propagator factor* with an exchange particle of mass m

$$\boxed{G = \frac{-1}{\mathsf{P}\cdot\mathsf{P} + m^2c^2}} \tag{1.46}$$

that contributes to the scattering amplitude. In the case of the Yukawa potential, it is easy to show that the propagator factor in (1.44) is the Green's function of the Klein-Gordan equation. The shorter range the interaction, the heavier the mass of the associated exchange particle; for the infinite-range electromagnetic interaction, this particle must be massless (the photon). g can now be interpreted as a *vertex factor* that measures the strength of the interaction or coupling of the exchange particle with other objects. There is one factor of g at the point of creation of the virtual particle, and another one at the point at which it is absorbed. We shall revisit these concepts in section 1.3.

1.2 Partial Wave Theory

An alternative approach to quantum mechanical scattering is that of *partial wave analysis*. As these (elastic) scattering events have azimuthal symmetry, the orbital angular momentum of the particles must be conserved. This means that we can decompose the incoming and outgoing waves as a superposition of states of well-defined angular momentum:

$$e^{i\mathbf{k}\cdot\mathbf{x}} = \sum_{\ell=0}^{\infty} i^{\ell}(2\ell+1)J_{\ell}(kr)P_{\ell}(\cos\theta) \tag{1.47}$$

where $J_\ell(kr)$ are the Bessel functions of the first kind, and $P_\ell(\cos\theta)$ are the familiar Legendre polynomials

$$P_0 = 1, \quad P_1 = \cos\theta, \quad P_2 = \frac{1}{2}(3\cos^2\theta - 1) \tag{1.48}$$

The radial Schrödinger equation then reads

$$\frac{d^2u_\ell}{dr^2} - \frac{\ell(\ell+1)}{r^2}u_\ell + \frac{2m}{\hbar^2}[E - V(r)]u_\ell = 0, \quad u_\ell(r) = rJ_\ell(kr) \tag{1.49}$$

As before, the aim is to solve this equation for a given scattering potential $V(r)$.

1.2.1 Partial Wave Scattering

As before, assume a localised potential ($Vr \to 0$ as $r \to \infty$). Far away from the scattering centre, the solutions must reduce approximately to plane waves. For this, we use the large argument limit of the Bessel functions

$$\lim_{r\to\infty} J_\ell(kr) = \frac{\sin\left(kr - \ell\frac{\pi}{2}\right)}{kr} = \begin{cases} \frac{\sin(kr)}{kr} & \text{for } \ell \text{ odd} \\ \frac{\cos(kr)}{kr} & \text{for } \ell \text{ even} \end{cases} \tag{1.50}$$

Adopting a solution of the form

$$\langle \mathbf{x}|\psi\rangle = \sum_{\ell=0}^{\infty} c_\ell J_\ell(kr)P_\ell(\cos\theta) \tag{1.51}$$

for constants c_ℓ, it can be shown that the associated scattering amplitude and differential cross section are given by

$$\boxed{\begin{aligned} f(\theta) &= \frac{1}{k}\sum_{\ell=0}^{\infty}(2\ell+1)P_\ell(\cos\theta)e^{i\delta_\ell}\sin\delta_\ell \qquad (1.52)\\ \sigma &= \frac{4\pi}{k^2}\sum_{\ell}(2\ell+1)\sin^2\delta_\ell \qquad (1.53)\end{aligned}}$$

δ_ℓ is the phase shift in the plane wave solution due to the potential for a given value of ℓ, which can be obtained through solving the radial Schrödinger equation with appropriate boundary conditions. We observe that a partial wave will have a small (large) contribution to the cross section if the phase shift is close to $n\pi$ (close to $\left(n+\frac{1}{2}\right)\pi$) for some integer n.

Consider (1.53). For elastic scattering, the phase shifts δ_ℓ must be real, meaning that

$$\sigma_\ell \leq \frac{4\pi}{k^2}(2\ell+1) \tag{1.54}$$

This is often referred to as the *unitarity limit*, which places an upper bound on the scattering cross sections for a given partial wave.

s-wave Scattering

As the wavefunctions in the scattering problem are not angular momentum eigenstates, the solution could - in principle - involve an infinite superposition of eigenstates of well-defined angular momentum, as in (1.51). This would not be particularly suited to analytical solution, and so we want to find a way to truncate the series.

For a plane wave of momentum $\mathbf{p} = \hbar\mathbf{k}$, the angular momentum associated with different parts correlates with the impact parameter b as $\mathbf{p} \cdot \mathbf{x} = \hbar kb$. Consequently, the part of the plane wave that is on axis will be dominated by the contribution from $\ell = 0$. For low energies, the plane waves will be concentrated close to the potential (on-axis), and so we often only consider the partial waves with $\ell = 0$, known as s-waves. For this to be a valid approximation, we must have that $ka \backsim kr \ll 1$, where a is some scale associated with the localised potential.

1.2.2 Delta-Sphere Scattering

As an example, we will consider scattering from a spherically symmetric delta-function potential of the form

$$V(r) = V_0\delta(r - a) \tag{1.55}$$

in the s-wave scattering regime. In this case, the radial Schrödinger equation becomes

$$-\frac{\hbar^2}{2m}\frac{d^2u}{dr^2} + V_0\delta(r - a)u = Eu \tag{1.56}$$

where we have written $u_0 \equiv u$. Integrating this equation from $r = a - \varepsilon$ to $r = a + \varepsilon$, for $\varepsilon \to 0$, yields:

$$\lim_{\varepsilon\to 0}\left.\frac{du}{dr}\right|_{a-\varepsilon}^{a+\varepsilon} = \frac{2mV_0}{\hbar^2}u(a) \tag{1.57}$$

This is our condition on the first derivative of our solution at the boundary. We adopt solutions of the form

$$u_1 = A\sin(kr + \delta_0)$$
$$u_2 = \sin(kr)$$

where δ_0 is the resultant phase, and u_1 and u_2 correspond to inside and outside the shell respectively. Matching these at the boundary $r = a$ and using (1.57), we obtain

$$A\sin(ka + \delta_0) = \sin(ka) \tag{1.58}$$

$$Ak\cos(ka + \delta_0) - k\cos(ka) = \frac{2mV_0}{\hbar^2}\sin(ka) \tag{1.59}$$

which can be combined to give

$$\cot(ka + \delta_0) - \cot(ka) = \frac{2mV_0}{\hbar^2}\frac{1}{k} \tag{1.60}$$

Now, in the s-wave regime, $ka \ll 1$, meaning that we can expand $\cot x \approx 1/x - x/3$, and it quickly follows that the resultant phase shift is given by

$$\delta_0 = -\frac{ka\Phi}{1 + \Phi}, \quad \Phi = \frac{2mV_0a}{\hbar^2} \tag{1.61}$$

From this, it is easy to find the resultant scattering amplitude and cross section using (1.52) and (1.53).

1.3 Feynman Diagrams

To deal with relativistic scattering processes that occur under some Hamiltonian H, we need to calculate the Lorentz-invariant scattering amplitude that connects the initial state $|\psi_i\rangle \equiv |i\rangle$ containing some particles of well defined momentum to a final state $|\psi_f\rangle \equiv |f\rangle$ containing another (often different) set of particles that also have well-defined momenta.

We can do this perturbatively through the use of *Feynman diagrams*. Each unique diagram corresponding to a given process shows a different way in which an interaction can occur, and represents a contribution to the transition matrix element $\mathcal{M}_{if} = \langle i| H |f\rangle$ from Fermi's Golden rule:

$$\boxed{\Gamma = \frac{2\pi}{\hbar} |\langle i| H |f\rangle|^2 \frac{dN}{dE_f}} \tag{1.62}$$

where E_f is the final energy state of the system. There are, in principle, an infinite number of possible diagrams. Incoming lines in a Feynman diagram have a well-defined momentum and energy; these represent the incoming and outgoing particles after some process. Since these diagrams represent transitions between well-defined states of four-momentum, they already include the contributions from all possible paths in both time and space through which the intermediate particles might have passed. This means that the time-orderings of the events is generally irrelevant. For a diagram to be distinct from another, it must feature a change in the way in which the lines are connected, rather than the apparent ordering. Generally, the incoming state is placed on the left-hand side, while the outgoing state is placed on the right-hand side; if you like, 'time' goes from left to right. For each internal line - that is, for each virtual particle - we can associate a propagator factor as in (1.46).

Vertices are places were particles are created or annihilated, with which we can associate a vertex factor that describes the strength of the interaction between the particles meeting there. If these vertex factors are small (such as in the electromagnetic and weak interactions), diagrams with a larger number of vertices make a smaller contribution to $\mathcal{M}_{if}$; it is for this reason that Feynman diagrams are a perturbative method of treating relativistic scattering processes. Diagrams with the lowest number of possible vertices for the process are said to be *first order* (or *tree-level*) diagrams, while those with another vertex are *second order* and so on.

Let us examine the vertex factor corresponding to the electromagnetic interaction via the photon. For interactions of photons with electrons, the vertex factor is of magnitude $-g_{\text{EM}}$, where g_{EM} is a dimensionless coupling constant. Recall the definition of the electromagnetic fine structure constant:

$$\alpha_{EM} = \frac{e^2}{4\pi\epsilon_0\hbar c} \approx \frac{1}{137} \tag{1.63}$$

For the electromagnetic force, the coupling strength must be proportional to the electric charge of the particle, meaning that a convenient choice of g_{EM} is

$$g_{EM} = \sqrt{4\pi\alpha_{EM}} = e/\sqrt{\epsilon_0\hbar c} \tag{1.64}$$

For interactions involving any particle of charge Q, the propagator factor is simply Qg_{EM}. The coupling constants for the other forces are defined similarly, and we note that $\alpha_W \approx 1/29$ and $\alpha_S \approx 1$. This means that we cannot easily apply the method of Feynman diagrams to strong interactions, as higher order diagrams are of comparable contributions to the first order ones.

Feynman diagrams are a way of representing a transition between an initial and final state of well-defined four-momentum, independent of the time ordering of the process that creates the transition.

The propagator and vertex factors present in the diagram are used to calculate the transition matrix element $\mathcal{M}_{if}$. The propagator factor associated with a virtual (off mass-shell) particle of mass m is given by

$$G = \frac{-1}{\mathsf{P}\cdot\mathsf{P} + m^2c^2}, \quad \mathsf{P}\cdot\mathsf{P} \neq -(E/c)^2 + \mathbf{p}^2 \tag{1.65}$$

Each force has a specific propagator and coupling constant, as follows

Force	Propagator	Notation	Vertex Factor
Electromagnetic	Photon γ	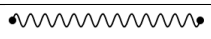	$g_{\mathrm{EM}}Q$
Weak	$W^{\pm}, Z^0$ Bosons		g_W
Strong	Gluon g	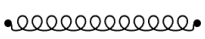	g_S

(1.66)

Fermions are represented with a solid line. Normal fermions have arrows going forward in time (generally left to right), while their corresponding anti-particle has an arrow pointing backwards in time. Alternatively, identifying the type of particle corresponding to a given line fixes the direction.

1.3.1 Common Diagrams

In this section, we note some of the common diagrams that one can encounter in the learning of subatomic physics. It is recommended that readers use these mainly for reference; the meaning of some of the diagrams will become clearer later on in this text. However, it is a useful exercise to examine these diagrams in order to gain an understanding of how they are constructed.

Electron-Positron Processes

- First order $e^+e^- \to e^+e^-$:

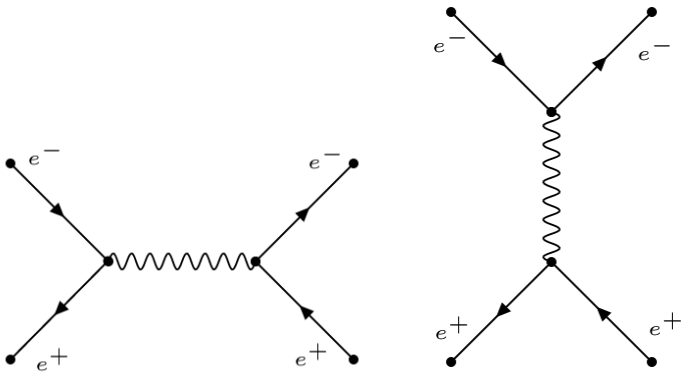

Figure 1.4: The first order Feynman diagrams for $e^+e^- \to e^+e^-$

- Some second order $e^+e^- \to e^+e^-$:

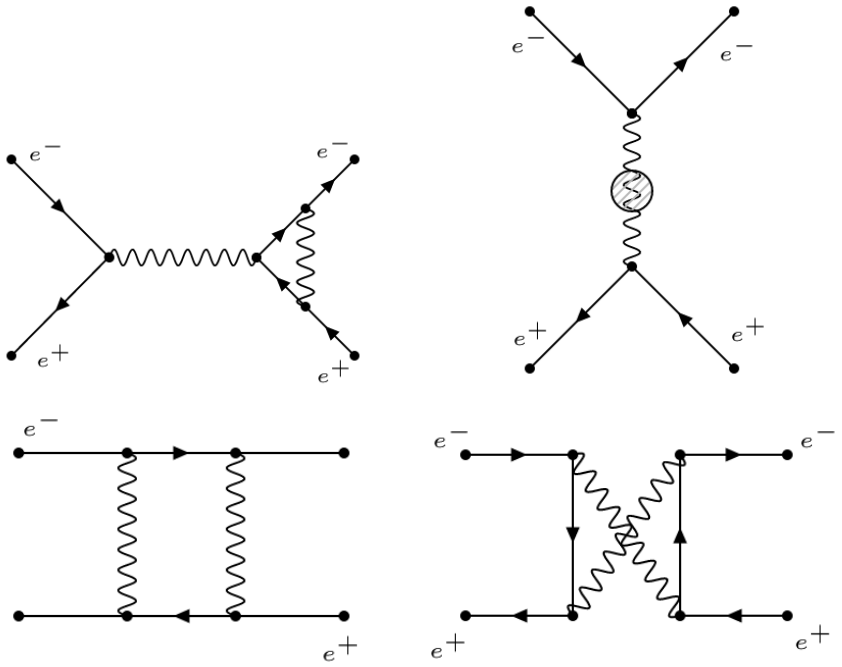

Figure 1.5: Some second order Feynman diagrams for $e^+e^- \to e^+e^-$

- Some third order Feynman diagrams for $e^+e^- \to e^+e^-$:

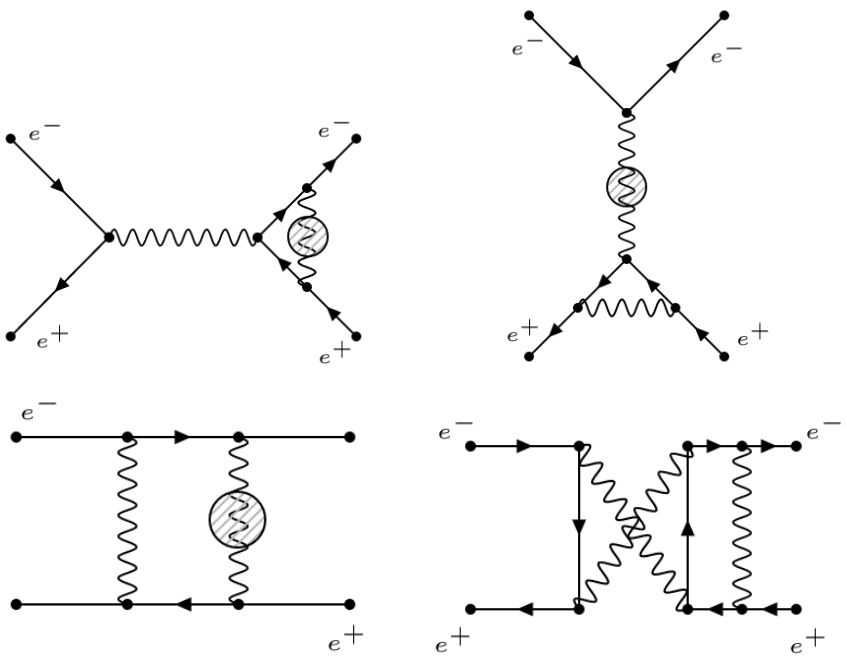

Figure 1.6: Some third order Feynman diagrams for $e^+e^- \to e^+e^-$

- First order $e^+e^- \rightarrow \mu^+\mu^-$:

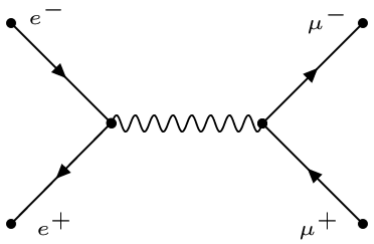

Figure 1.7: The first order Feynman diagram for $e^+e^- \rightarrow \mu^+\mu^-$

- First order $e^+e^- \rightarrow$ hadrons:

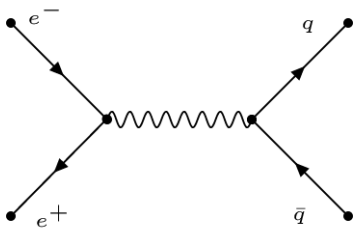

Figure 1.8: The first order Feynman diagram for $e^+e^- \rightarrow$ hadrons

Electron-Electron Processes

- First order $e^-e^- \rightarrow e^-e^-$:

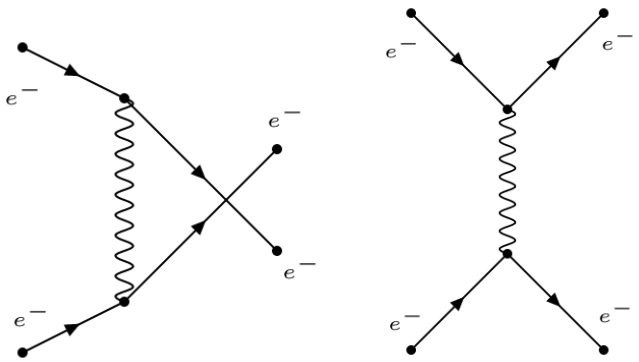

Figure 1.9: The first order Feynman diagrams for $e^-e^- \rightarrow e^-e^-$

- Some first order $e^-e^- \rightarrow e^-e^- + \mu^+\mu^-$:

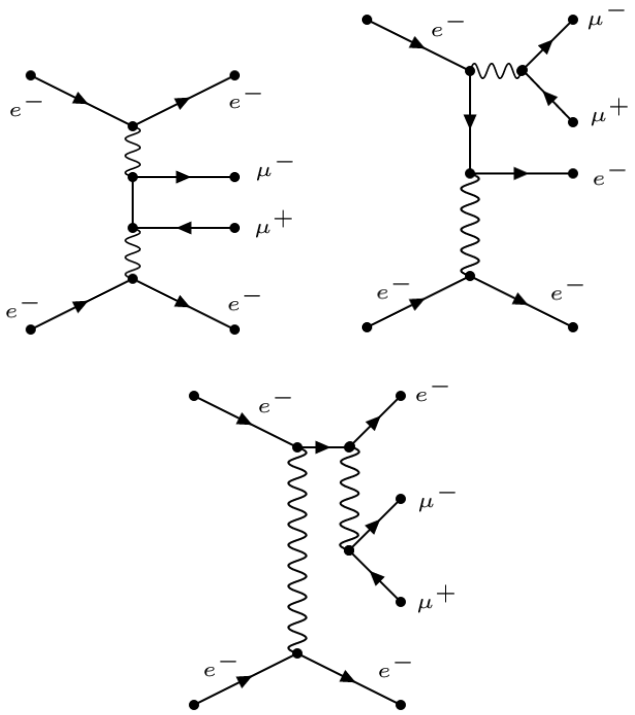

Figure 1.10: Some first order Feynman diagrams for $e^-e^- \rightarrow e^-e^- + \mu^+\mu^-$

Photon Processes

- One (of two) first order $\gamma \rightarrow e^+e^-$:

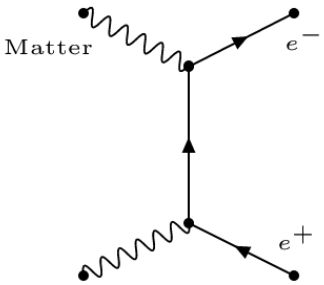

Figure 1.11: A first order Feynman diagram for $\gamma \rightarrow e^+e^-$. Note that the interaction with matter is required in order for this process to occur

- First order $\gamma\gamma \rightarrow \gamma\gamma$:

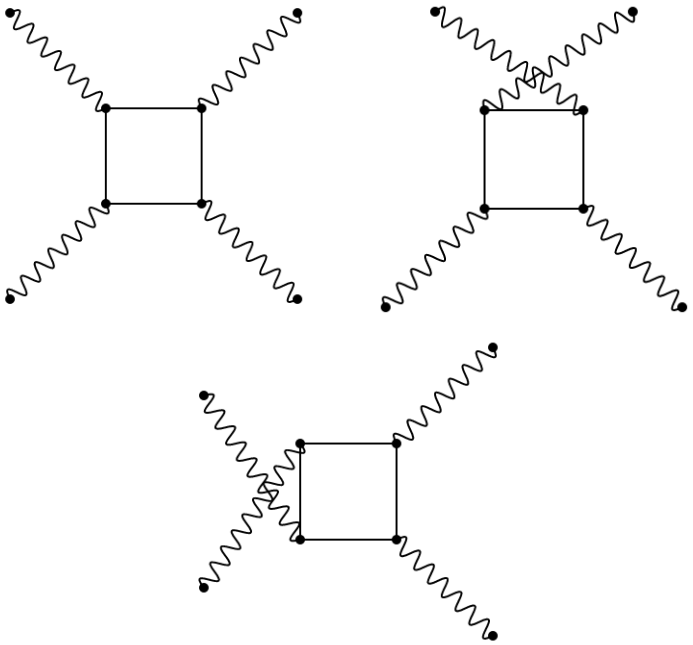

Figure 1.12: The first order Feynman diagrams for $\gamma\gamma \rightarrow \gamma\gamma$

Decay Processes

- Beta-minus decay:

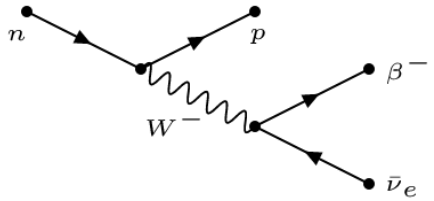

Figure 1.13: The first order Feynman diagram for beta-minus decay

- Beta-plus decay:

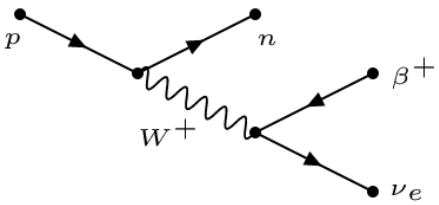

Figure 1.14: The first order Feynman diagram for beta-plus decay

- μ^- lepton decay:

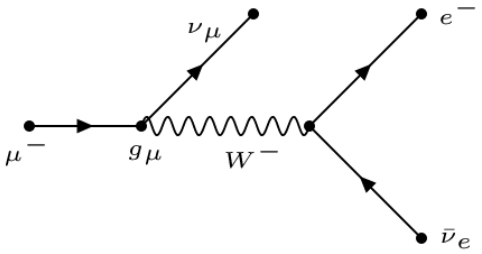

Figure 1.15: The first order Feynman diagram for μ_- decay

- τ^- lepton decay:

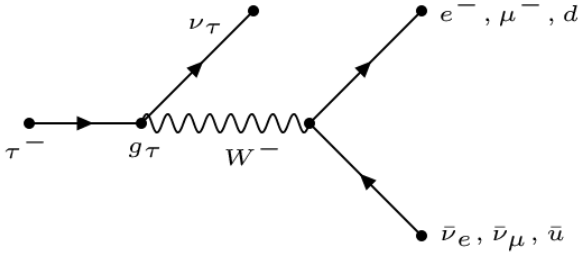

Figure 1.16: The first order Feynman diagram for τ_- decay

Note that for the last two decays, hadronic decays are only possible in the τ^- case as the μ^- is not massive enough to produce hadrons.

1.3.2 Analysing Feynman Diagrams

Let us now take a look at an example of calculating the collision cross section corresponding to a Feynman diagram. Suppose that we observe the following process:

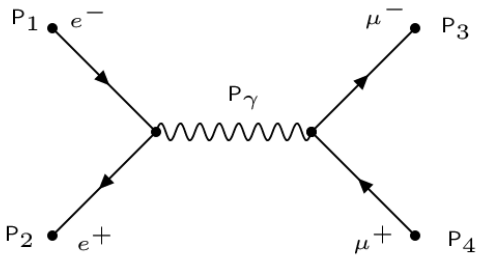

Figure 1.17: First order Feynman diagram for the process $e^+e^- \rightarrow \mu^+\mu^-$ with four-momenta shown

In the centre of mass frame of the two electrons, the four momenta are given by

$$\mathsf{P}_1 = (E_e/c, \mathbf{p}), \quad \mathsf{P}_2 = (E_e/c, -\mathbf{p}), \quad \mathsf{P}_\gamma = \mathsf{P}_1 + \mathsf{P}_2 = (2E_e/c, 0) \tag{1.67}$$

As $m = 0$ for a photon, the associated propagator is $c^2/4E_e^2$. The relevant matrix element is then calculated from

$$\mathcal{M}_{if} = \hbar^3 c \times \text{Propogators} \times \text{Vertex factors} = g_{\text{EM}}^2 \frac{\hbar^3 c^3}{4E_e^2} \tag{1.68}$$

The differential cross section is calculated by dividing the transition rate (as predicted by Fermi's golden rule (1.62)) by the incoming flux $j = 2v_e = 2c^2 p_e/E_e$:

$$d\sigma = \frac{E_e}{2c^2 p_e} \frac{2\pi}{\hbar} |\mathcal{M}_{if}|^2 \frac{dN}{dE_f} \tag{1.69}$$

Overall momentum conservation implies that only one of the particles contributes to the density of states, vis.:

$$\frac{dN}{dE_f} = \frac{dN}{dp_\mu} \frac{dp_\mu}{dE_f} = \frac{4\pi}{(2\pi\hbar)^3} p_\mu^2 \frac{dp_\mu}{dE_f} \tag{1.70}$$

In the centre of mass frame, $E_\mu \gg m_\mu c^2$, such that $E_\mu \approx \frac{1}{2} E_f$. Since these muons are on external legs, they are on mass shell, such that

$$E_\mu^2 = p_\mu^2 c^2 + m_\mu^2 c^4 \quad \longrightarrow \quad E_\mu dE_\mu = c^2 p_\mu dp_\mu \tag{1.71}$$

meaning that we can write

$$\frac{dp_\mu}{dE_f} = \frac{1}{2} \frac{dp_\mu}{dE_\mu} = \frac{1}{2c^2} \frac{E_\mu}{p_\mu} \tag{1.72}$$

Substituting everything into (1.69), and integrating over the solid angle,

$$\sigma = \pi \hbar^2 c^2 \frac{\alpha_{\text{EM}}^2}{s}, \quad s = (2E)^2 \tag{1.73}$$

where we have used the fact that $\alpha_{\text{EM}} = g_{\text{EM}}^2/4\pi$. Note that s is simply the square of the centre of mass energy. These sorts of calculations are often done in naturalised units

1.4 Resonances

Sometimes the projectile used in a scattering experiment can be absorbed by the target to form a compound state, and then later re-emitted. The time-energy uncertainty relationship from quantum mechanics tells us that if a state has only a finite lifetime $\Delta t \backsim \Gamma^{-1}$, then the uncertainty on its energy is given by

$$\Delta E \Delta t \backsim \hbar \quad \longrightarrow \quad \Delta E \backsim \hbar\Gamma \tag{1.74}$$

This means that if we take a set of identical unstable particles, and measure the mass of each, we will expect to get a range of values with width of order $\Gamma\hbar/c^2$. Long-lived intermediate states have small Γ, and hence well-defined energies. We tend to think of these long lived states as 'particles', such as the neutron. Short-lived intermediate states have large width, and less-well defined energies. When the intermediate state is so short lived that $\Gamma\hbar/c^2$ is comparable to the mass, then the decay is so rapid that it is no longer useful to think of it as a particle; it is really just a transitional state.

1.4.1 Resonant Scattering

Let us return to partial wave theory, and have a look at what happens to the collision cross section σ close to resonance, where the phase shift $\delta_\ell \approx \left(n + \frac{1}{2}\right)\pi$. Expand around the resonance energy E_0:

$$\cot\delta_\ell(E) \approx \underbrace{\cot\delta_\ell(E_0)}_{=0} + \left.\frac{d\cot\delta_\ell}{dE}\right|_{E=E_0}(E-E_0) + \dots \tag{1.75}$$

We define

$$\left.\frac{d\delta_\ell}{dE}\right|_{E=E_0} = \frac{2}{\Gamma} \tag{1.76}$$

such that our expansion becomes

$$\cot\delta_\ell(E) \approx -\underbrace{\frac{1}{\sin\delta_\ell^2}}_{=1}\left.\frac{d\delta_\ell}{dE}\right|_{E=E_0}(E-E_0) + \dots \approx -\frac{2}{\Gamma}(E-E_0) \tag{1.77}$$

The collision cross-section is then

$$\sigma_\ell = \frac{4\pi}{k^2}(2\ell+1)\sin^2\delta_\ell = \frac{4\pi}{k^2}(2\ell+1)\frac{1}{1+\cot^2\delta_\ell} \approx \frac{4\pi}{k^2}(2\ell+1)\frac{\Gamma^2/4}{(E-E_0)^2+\Gamma^2/4} \tag{1.78}$$

Introducing the appropriate degeneracy factors, and taking into account that the resonance may decay into a final or initial state, we arrive at

$$\boxed{\sigma = \frac{4\pi}{k^2}\frac{2j+1}{(2s_1+1)(2s_2+1)}\frac{\Gamma_i\Gamma_f/4}{(E-E_0)^2+\Gamma^2/4}} \tag{1.79}$$

This is known as the *Breit-Wigner formula* for resonant scattering, and has the following features:

- Γ_i is the *partial width* of the resonance to decay to the initial state
- Γ_f is the *partial width* of the resonance to decay to the final state
- $\Gamma = \sum_j \Gamma_j = \tau^{-1}$ is the *full width* of the resonance at half-maximum (Γ_j are all the possible decays)
- E is the centre of mass energy of the system
- E_0 is the characteristic rest mass energy of the resonance
- j is the total angular momentum of the resonance, while s_1 and s_2 are the initial spin angular momenta of the two particles used to create the resonance
- k is the wavenumber of the incoming particles in the centre of mass frame, which is equal to its momentum in natural units

The cross section is non-zero at any energy, but has a sharp peak when E is close to E_0 (Lorentzian shape). Longer lived resonances have smaller Γ and hence sharper peaks. It is also useful to define the branching ratio

$$B_j = \frac{\Gamma_j}{\Gamma} \tag{1.80}$$

that represents the fraction of the time that the resonance will decay into a particular state. These are determined empirically.

2. *Nuclear Physics*

This chapter aims to cover the basic concepts of nuclear physics, including:

- The Structure of the Nucleus
- Decay Modes
- Nuclear Fusion and Fission

Now that we have a relatively in-depth understanding of scattering theory, we can now look at some of its consequences when applied to the structure of the nucleus. We shall also investigate the physics behind the various decay processes that the nucleus can undergo.

2.1 The Structure of the Nucleus

As stated previously, the experimental differential cross section for alpha particle scattering on nuclei departs from that predicted by the (point charge) Rutherford differential cross section (1.11) at higher alpha particle energies. This implies that there is some internal structure to the nucleus, as at these energies, the de-Broglie wavelength of the incident particles is comparable to the internal scales of the nucleus, allowing interaction. The form-factors (see (1.38)) obtained from experiments performed at higher energies can be modelled via the *Saxon-Woods potential*:

$$\boxed{\rho(r) = \frac{\rho_0}{1 + e^{-(r-a)/d}}} \tag{2.1}$$

a is the radius of the nucleus, while d is the thickness of the edge region over which the distribution drops off. It is important to note that this distribution is both spherically symmetric, and very similar to that of a hard sphere for small d.

2.1.1 The Nuclear Interaction

We now know that nuclei consist of protons ($m_p = 983.3\,\mathrm{MeV}/c^2$) and neutrons ($m_n = 989.6\,\mathrm{MeV}/c^2$). We usually denote individual nuclei as

$$^{A}_{Z}\mathrm{X} \tag{2.2}$$

where X is the chemical symbol of the element, Z is the corresponding *atomic number*, while A is the mass number of the particular isotope. Note that for some neutron number N, it is obvious that $A = Z + N$.

Performing scattering experiments with a number of nuclei of different mass numbers yields the following empirical relationship for the radius of the nucleus a

$$\boxed{r = r_0 A^{1/3}, \quad r_0 \approx 1.2\,\mathrm{fm}} \tag{2.3}$$

where A is the mass number as above. This has a number of implications for the nuclear force:

- The fact that r is proportional to $A^{1/3}$ indicates that the volume of the nucleus $V \propto r^3$ is proportional to the mass number A, meaning that each *nucleon* (proton or neutron) is making an equal contribution to the overall volume. This means that we only have to take into account nearest-neighbour interactions between nucleons
- There must be a repulsive force/core to the inter-nucleon potential in order to prevent the collapse of the nucleus. This is provided by Pauli exclusion
- The inter-nuclear force must be very strong at short distances to overcome the electrostatic repulsion between the protons, but vanishingly small at distances $\backsim 2r_0$ as we observe no effect of the nuclear force on the electronic structure of atoms. This implies the existence of massive exchange particles ($\pi^0, \pi^{\pm}$)

We shall later see that the nuclear force is a residual effect of the strong force between the quarks that make up the protons and neutrons within the nucleus.

2.1.2 The Semi-Empirical Mass Formula

When calculating the mass of the nucleus ($\backsim$ GeV/c^2), we must take into account the binding energy between the nucleons, as this will represent a sizeable correction to the mass ($\backsim$ MeV/c^2). As such, we propose the *Semi-empirical mass formula (SEMF)*

$$M(A,Z)c^2 = Zm_pc^2 + (A-Z)m_nc^2 - B(A,Z) \tag{2.4}$$

$$B(A,Z) = \underbrace{a_V A}_{\text{Volume}} - \underbrace{a_S A^{2/3}}_{\text{Surface}} - \underbrace{a_A \frac{(N-Z)^2}{A}}_{\text{Asymmetry}} - \underbrace{a_C \frac{Z^2}{A^{1/3}}}_{\text{Coulomb}} \pm \underbrace{\delta(N,Z)}_{\text{Pairing}} \tag{2.5}$$

where $a_V, a_s, a_A, a_C, \delta$ are all constants. Let us examine the origin and consequences of the various terms within the binding energy:

- Volume and Surface terms - The properties of the inter-nuclear force detailed above are similar to the forces between molecules in an incompressible liquid. The energy of such a 'liquid-drop' is $E = -c_1 n + 4\pi R^2 T$ for a number density n and surface tension T. Recognising that $R \propto n^{1/3}$, and that $n \backsim A$, we obtain the above two terms

- Asymmetry term - Pauli exclusion dictates that neither protons nor neutrons can occupy the same quantum state as other neutrons or protons. However, it is possible for a proton and a neutron to exist in the same state, since the particles are not identical. The asymmetry term thus arises from the Fermi statistics of the nucleons, as an inbalance in the energy of the occupied states will increase the total energy of the nucleus. A detailed calculation can be found in the next section. This term will thus favour nuclei in which $N = Z$

- Coulomb term - As there is Coulomb repulsion within the nucleus, we must include a term of the form Z^2/r. As $r \backsim A^{1/3}$, we can write a term of the above form. The coulomb term favours neutral nuclei

- Pairing term - This is due to the spin states of the nucleons, as they tend to couple pair-wise (n-n or p-p) to more stable configurations. This means that nuclei with an even number of nucleons will be more tightly bound that those with an odd number. Thus, even-even (N-Z) nuclei have $+\delta$, even-odd or odd-even nuclei have 0 contribution, and odd-odd nuclei have $-\delta$

Being a semi-empirical law, the constants in the SEMF are determined by experiment. However, the exact values depend on the way in which the fitting is done on the experimental data. One such set of values is:

Volume	Surface	Asymmetry	Coulomb	Pairing
a_V	a_S	a_A	a_C	δ
15.835	18.33	23.2	0.71	$11.2/\sqrt{A}$

Table 2.1: Values of the constants in the SEMF

The SEMF is remarkably accurate for elements with $A \gtrsim 30$, with the exception of a few regions close to 'magic' numbers of A and Z. For $A \lesssim 30$, many of the assumptions made in deriving the formula begin to break down. For example, at low A, we can no longer assume that $(N-Z) \ll A$, meaning that the asymmetry term begins to dominate, favouring $N = Z$. It correctly predicts the maximum binding energy per nucleon as occurring around Fe or Ni.

The Asymmetry Term

We can derive the explicit form for the asymmetry term by considering the nucleons to be a degenerate Fermionic gas, with mean occupation numbers

$$\bar{n}_i = \frac{1}{e^{\beta(E-\mu)} - 1} \tag{2.6}$$

For these calculations, we shall assume that $m_p \approx m_n \equiv m$. Assuming that the nucleons are non-relativistic (a pretty safe assumption), such that we can adopt the usual energy dispersion relation

$$E = \frac{p^2}{2m} = \frac{\hbar^2 k^2}{2m} \tag{2.7}$$

such that the density of states becomes

$$g(E)dE = \frac{(2s+1)Vm^{3/2}}{\sqrt{2}\pi^2\hbar^3} E^{1/2} dE \tag{2.8}$$

Then, we can determine E_F as the analytic solution to some equation for N, the number of nucleons of a specific species within the system, remembering that $\bar{n}_i$ behaves as a step-function for $E \ll E_F$ (it is easy to show that this is satisfied in the nucleus):

$$N = \sum_n \bar{n}_i = \int_0^{E_F} dE\, g(E) = \frac{(2s+1)Vm^{3/2}}{\sqrt{2}\pi^2\hbar^3} \frac{2}{3} E_F^{3/2} \tag{2.9}$$

Rearranging, we find that the Fermi energy is given by

$$E_F = \left(\frac{6\pi^2 n}{2s+1}\right)^{2/3} \frac{\hbar^2}{2m} \tag{2.10}$$

It follows that the mean energy is given by

$$\langle E \rangle = \sum_i \bar{n}_i E_i = \int_0^{E_F} dE\, g(E) E = \frac{3}{5} N E_F \tag{2.11}$$

For the entire nucleus, the mean energy is the sum of the mean energies of each species. Consider the case where $N = Z = A/2$. Then, the Fermi energy for both species is given by

$$E_F = \frac{\hbar^2}{2m}\left(\frac{3\pi^2 N}{V}\right)^{2/3} = \frac{\hbar^2}{2mr_0^2}\left(\frac{9\pi}{8}\right)^{2/3} \tag{2.12}$$

where we have used the fact that $V = (4\pi/3)r^3 = (4\pi/3)r_0^3 A$ as per (2.3). In the case that $N \approx Z$, we have that

$$\langle E \rangle = \langle E_N \rangle + \langle E_Z \rangle = \frac{3}{5} E_F \frac{N^{5/3} + Z^{5/3}}{(A/2)^{2/3}} \tag{2.13}$$

Let $\delta = (Z-N)/A$, such that $N = A(1-\delta)/2$ and $Z = A(1+\delta)/2$. As δ is small, we can expand $(1 \pm x)^{5/3} \approx 1 \pm \frac{5}{3}x + \frac{1}{2!}\frac{5}{3}\left(\frac{5}{3} - 1\right)x^2$. Collecting like terms, we find that the asymmetry term must be given by

$$E_{\text{asymmetry}} = \frac{1}{3} E_F \frac{(N-Z)^2}{A} \tag{2.14}$$

Evaluating the pre-factor, we find that $E_F/3 \approx 11.2\,\text{MeV}$, just under half of the value observed experimentally in table 2.1. This is due to the fact that we have not taken into account the effect that the occupation symmetry has on the potential energy of the nucleus.

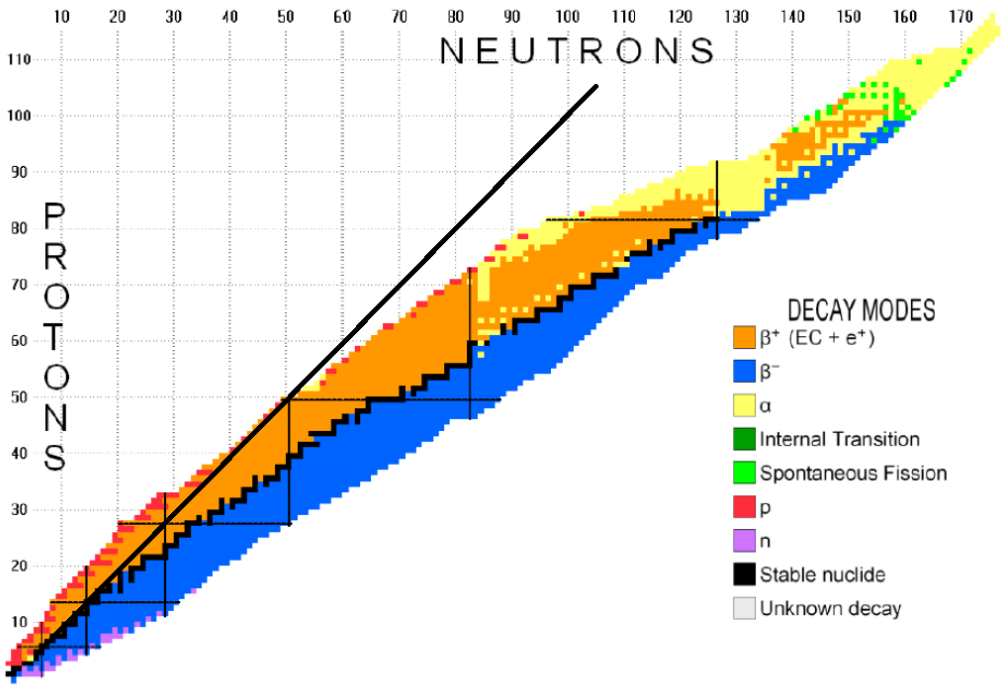

Figure 2.1: Decay modes of the nuclei plotted in the N-Z plane. The line of $N = Z$ is shown (solid)

The N-Z plane

If we look at elements in the N-Z plane, we observe that the naturally occurring isotopes (both stable and unstable) at first follow the $Z = N$ line, and then become neutron rich at larger A. Stable isotopes occur close to the center of the band, while unstable isotopes are closer to the perimeter. The SEMF can re-produce this dependence, if we maximise the binding energy $B(A, Z)$ with respect to Z for a given A:

$$\left(\frac{\partial B}{\partial Z}\right)_A = -a_A \frac{2(A-2Z)(-2)}{A} - a_C \frac{2Z}{A^{1/3}} = 0 \tag{2.15}$$

Re-arranging, this becomes

$$\boxed{\frac{N}{Z} = 1 + \frac{a_C}{2a_A} A^{2/3}} \tag{2.16}$$

This is the equation for the *valley of stability* in the N-Z. Note that there are no stable isotopes beyond ^{208}Pb, as they are too massive to remain stable. Figure 2.1 shows this dependence, and also shows the ways in which the various isotopes decay towards the valley of stability, as we shall investigate in the next section.

2.2 Decay Modes

As stated previously, nuclei will tend towards configurations which maximise the binding energy per nucleon. In order to do so, they will undergo nuclear decay processes. The available energy for such a process is given by the difference between the rest mass energy of the initial and final constituents of the system:

$$\boxed{Q/c^2 = \sum_i M_i(A,Z) - \sum_f M_f(A,Z)} \tag{2.17}$$

This is known as the *Q-value*. If $Q > 0$, then the decay process is energetically favourable, and allowed classically. After the decay, this energy is carried away by one or more of the decay products.

2.2.1 Radioactive Decay Law

All readers of this text will be familiar with the radioactive decay law for a species of population N:

$$\frac{dN}{dt} = -\Gamma N \tag{2.18}$$

The constant Γ is the decay rate per-nucleus. For a single species, this equation is easily integrated to give

$$N(t) = N_0 e^{-\Gamma t} \tag{2.19}$$

We can calculate the particles' mean proper lifetime τ, using the fact that the probability that they decay in the interval $[t, t+dt]$ is

$$P(t)dt = -\frac{1}{N_0}\frac{dN}{dt}dt = \Gamma e^{-\Gamma t}dt \tag{2.20}$$

The mean lifetime is then

$$\tau = \langle t \rangle = \frac{\int_0^\infty dt\, tP(t)}{\int_0^\infty dt\, P(t)} = \frac{1}{\Gamma} \tag{2.21}$$

as one would expect. For a system of coupled decay species A, B and C, we can define $\mathbf{N} = (A, B, C)^T$, such that

$$\frac{d\mathbf{N}}{dt} = R\mathbf{N} \tag{2.22}$$

where R is a 'rate matrix' containing the decay rate coefficients. The general solution is then given by

$$\mathbf{N} = \mathbf{N}(0)e^{Rt}, \quad e^{Rt} = Ue^{t\widehat{R}}U^{-1} \tag{2.23}$$

where $\widehat{R}$ is the diagonalised form of R, and U consisting of the eigenvectors of R as column vectors. Let hope you haven't forgotten the definition of the exponential matrix.

This radioactive decay law assumes that the decay rate is independent of the decay history of the nucleus (delta correlated in time), the method of preparation of the nucleus, and its environment. It also assumes that the nucleus decays via a single process at a given rate Γ, and that N is sufficiently large that this rate remains roughly constant over many decay lifetimes. These approximations are valid provided that $m \gg \Gamma\hbar/c^2$, as this means that we can consider the constituents of the nucleus to be particles.

2.2.2 Alpha Decay

In alpha decays, the nucleus ejects a ${}^4_2\mathrm{He}$ nucleus (α particle), meaning that the process can be written as

$$\boxed{{}^A_Z\mathrm{X} \longrightarrow {}^{A-4}_{Z-2}\mathrm{Y} + {}^4_2\mathrm{He}} \tag{2.24}$$

In order for this process to occur, it must tunnel through the potential barrier that is present due to the combination of the nuclear and electrostatic potentials. The radial Schrödinger equation for such a particle of energy Q is

$$\left(-\frac{\hbar^2}{2m}\frac{\partial^2}{\partial r^2} + V(r)\right)\langle \mathbf{x}|\psi\rangle = Q\,\langle \mathbf{x}|\psi\rangle \tag{2.25}$$

Without loss of generality, we can write this spherically symmetric wavefunction as the exponential of some other function $\exp\eta(r)$. After substituting this in, and dividing by $\exp\eta$, we obtain the differential equation

$$Q = -\frac{\hbar^2}{2m}\left[\eta'' + (\eta')^2\right] + V(r) \tag{2.26}$$

where the primes denote derivatives with respect to r. We can model the potential $V(r)$ felt by any α particle by

$$V(r) = \begin{cases} \text{constant} & \text{for } r < R_a \\ Z_1 Z_2 \frac{\hbar c \alpha_{\mathrm{EM}}}{r} & \text{for } r > R_a \end{cases} \tag{2.27}$$

Within the barrier, the potential is smoothly varying, so η should be a smoothly varying function in r. We then expect that $\eta'' \ll (\eta')^2$, and so we can safely neglect the former term in comparison to the latter. The tunnelling probability is given by the ratio of the mod-squared amplitudes:

$$P = \frac{|\langle R_b|\psi\rangle|^2}{|\langle R_a|\psi\rangle|^2} = e^{-2G} \tag{2.28}$$

where G is the *Gamow factor* given by

$$\boxed{G = \sqrt{\frac{2m}{\hbar^2}}\int_{R_a}^{R_b} dr\,\sqrt{V(r) - Q}, \quad R_a \approx r_0 A^{1/3}, \quad R_b = \frac{Z_1 Z_2 \hbar c \alpha_{\mathrm{EM}}}{Q}} \tag{2.29}$$

The inner limit R_a is an approximate value for the radius of the nucleus, while the outer limit R_b represents the critical radius at which the energy of the ejected particle is equal to the potential energy. As in many cases $Q \ll V$, we can evaluate this integral straightforwardly using (2.27) as

$$G \approx \sqrt{\frac{2m}{\hbar^2}}\sqrt{Z_1 Z_2 \hbar c \alpha_{\mathrm{EM}}}\int_{R_a}^{R_b} dr\, r^{-1/2} \approx \frac{Z_1 Z_2 e^2 \sqrt{2m}}{2\pi\epsilon_0\sqrt{Q}} \tag{2.30}$$

where we have neglected the contribution from the lower bound in the integral as $R_a/R_b \backsim Q \ll 1$. For α decay, $Z_1 = 2$ and $Z_2 \equiv Z$, where Z is the atomic number of the decay product. As the decay rates are given by $\Gamma = \Gamma_0 e^{-2G}$, it follows that

$$\boxed{\log\Gamma = A - \frac{BZ}{\sqrt{Q}}} \tag{2.31}$$

where again Z is the atomic number of the decay product, and A and B are constants. This is well behaved in the limits $Q \to 0$ and $Q \to \infty$. Note that this formula will predict lower decay rates (and branching ratios) for decays from atoms with non-zero values of angular momentum, as this will create some new V_{eff} that we have to use in our calculation of the Gamow factor by adding an extra term of the form $\ell(\ell+1)/(2mr^2)$.

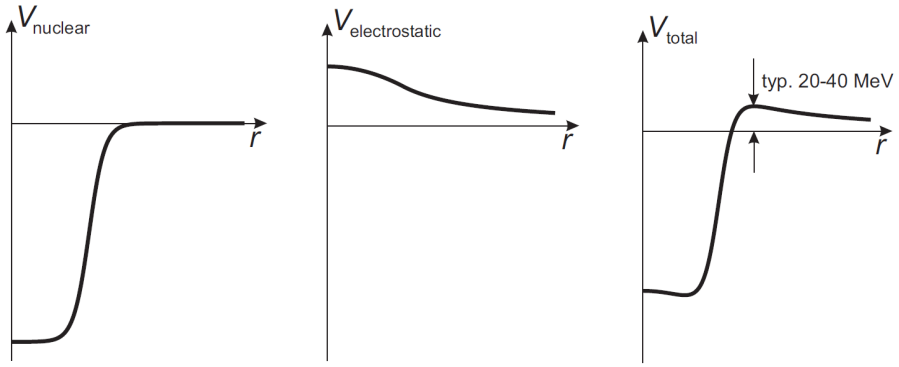

(a) (b) (c)

Figure 2.2: The potentials involved in alpha decay processes: (a) Nuclear potential (inverted Saxon-Woods shape) (b) Electrostatic potential (c) Combined potential

2.2.3 Weak Decays

There are three related nuclear decay processes which are all mediated by the weak interaction. These are as follows:

1. β^- decay (beta decay) - Neutron rich isotopes reduce N by emitting an electron and electron neutrino:

$$\boxed{{}^A_Z\mathrm{X} \longrightarrow {}^A_{Z+1}\mathrm{Y} + e^- + \bar{\nu}_e} \tag{2.32}$$

   Observation of this process allowed Pauli to postulate the existence of the neutrino, as it was required to satisfy both energy-momentum conservation, and spin-angular momentum conservation

2. β^+ decay (positron emission) - An isotope with a surplus of protons can emit a positron in order to replace one of the protons with a neutron:

$$\boxed{{}^A_Z\mathrm{X} \longrightarrow {}^A_{Z-1}\mathrm{Y} + e^+ + \nu_e} \tag{2.33}$$

3. Electron capture - An isotope with a surplus of protons can also remove one of the atomic electrons:

$$\boxed{{}^A_Z\mathrm{X} + e^- \longrightarrow {}^A_{Z-1}\mathrm{Y} + \nu_e} \tag{2.34}$$

   Both β^+ decay and electron capture result in the same changes to the nucleus, and so are 'competing' decay process. When considering which process is dominant, we note that the Q value is $2m_ec^2$ for electron capture is greater than for positron emission, but electron capture relies on there being substantial overlap between the wavefunctions of the nucleus and the atomic electrons

When viewed at the level of the nuclear constituents, all three of the above decays involve the interaction of four particles: a proton, a neutron, an (anti-)electron and an (anti-)neutrino. Only β^- decay can occur in isolation - as it is the only process with $Q > 0$ in the absence of binding energies - while the others have to occur inside the nucleus in order for $Q > 0$.

All of these processes leave the mass number A unchanged, meaning that the parent and daughter nuclei are isobars; these processes allow transitions between isobars. Odd-A nuclei only have one stable isobar (for which the mass of the system is minimised), while

even-A nuclei may have more than one isobar; an odd-odd (upper) and even-even (lower) isobar separated by 2δ from (2.5). This implies that more than one stable isobar can exist, provided that they occur at the minimum of the binding energy curves.

Fermi Theory of Beta Decay

We can apply Fermi's golden rule (1.62) to these decay processes. Let us consider the particular case of β^- decay, and make the following simplifying assumptions:

- That the four-body interactions all occur at a single point (vertex), which which we can associate the *Fermi coupling constant*, given by

$$G_F \approx 1.17 \times 10^{-5}\ \text{GeV}^{-2} \tag{2.35}$$

- In using a single coupling constant, we have implicitly made the assumption that the four-body interaction does not depend on the spin states of the incoming or outgoing particles

- That the wave-functions of the electron and anti-neutrino can be represented by plane waves.

$$\langle \mathbf{x}|\phi_e\rangle \equiv \phi_e = e^{i\mathbf{p}_e\cdot\mathbf{x}/\hbar}, \quad \langle \mathbf{x}|\phi_\nu\rangle \equiv \phi_\nu = e^{i\mathbf{p}_\nu\cdot\mathbf{x}/\hbar} \tag{2.36}$$

  This ignores the effect of the Coulomb interaction between the electron and the nucleus, which is a good approximation provided that the electron is sufficiently energetic

- That the nucleus is very massive in comparison to the electron and neutrino, which is almost always the case. This gives rise to the condition that

$$E_e + E_\nu = Q \tag{2.37}$$

The initial state is the state of the parent nucleus, while the final state is the product state of the daughter nucleus, electron state and anti-neutrino state:

$$|\Psi_i\rangle = |\psi_i\rangle\,, \quad |\Psi_f\rangle = |\psi_f\rangle \times |\phi_e\rangle \times |\phi_\nu\rangle \tag{2.38}$$

The transition matrix element is thus given by

$$\mathcal{M}_{if} = \langle \Psi_f|\, H\, |\Psi_i\rangle = G_F \int d^3\mathbf{x}\, \phi_e^*\phi_\nu^*\psi_f^*\psi_i \tag{2.39}$$

We can approximate this integral by remarking that $\mathbf{p}\cdot\mathbf{x} \ll 1$ on scales of the nucleus, meaning that to first order

$$\mathcal{M}_{if} \approx G_F \int d^3\mathbf{x}\, \psi_f^*\psi_i \equiv G_F M_{\text{nucl}} \tag{2.40}$$

M_{nucl} is the *nuclear matrix element* that denotes the integral overlap between the parent and daughter nucleus. In the case of the decay of the isolated neutron, the initial state neutron and final state proton occupy the same state, meaning that $|M_{\text{nucl}}| = 1$. Including higher order terms in the expansion of the plane waves leads to the suppression of transitions that do not have $|j - j'| \leq 1$ as the matrix elements evaluate to zero (selection rules).

We now need to calculate the density of states. As stated previously, we ignore the contribution from the daughter nucleus as it does gain any kinetic energy in the reaction. The partial number density is then given by

$$d^2N = \frac{d^3\mathbf{p}_e}{(2\pi\hbar)^3}\frac{d^3\mathbf{p}_\nu}{(2\pi\hbar)^3} = \frac{p_e^2 p_\nu^2}{4\pi^4\hbar^6} dp_e dp_\nu \tag{2.41}$$

where the second expression follows from assuming system isotropy. We want to integrate our the dependence of this expression on the momentum of the anti-neutrino. Approximating it as massless, (2.37) allows us to write that

$$dN = \frac{p_e^2}{4\pi^4\hbar^6}dp_e\,\frac{1}{c^3}\int dE_\nu\, E_\nu^2\delta(E_e + E_\nu - Q) = \frac{p_e^2(Q-E_e)^2}{4\pi^4\hbar^6c^3}dp_e dE_\nu \tag{2.42}$$

Remarking, again by (2.37), that $dE_f = dQ = dE_\nu$, we can thus write the final transition rate as

$$\boxed{\Gamma(p_e)dp_e = \frac{G_F^2\left|M_{\text{nucl}}\right|^2}{2\pi^3\hbar^7c^3}F(Z_D,p_e)p_e^2(Q-E_e)^2dp_e} \tag{2.43}$$

where $F(Z_D, p_e)$ is the *Fermi factor* that describes the correction due to the electromagnetic interaction between the electron and the daughter nucleus. For an isolated neutron decay, this simply contributes a factor of unity. It is easy to show (by integrating up to the maximum momentum) that for relativistically ejected particles, $\Gamma \propto Q^5$. This is sometimes known as *Sargent's rule*.

2.2.4 Gamma Decay

Gamma decays involve the emission of high energy ($\backsim$ MeV) photons from a nucleus due to the relaxation of excited nuclear states. These processes are usually associated with a preceding α or β decay, as these often leave the nucleus in an excited state. Gamma decays are usually quite rapid due to the short relaxation time of such nuclei. As γ decays involve transitions between states of well-defined energy in the nucleus, the energy of the resultant photons are well-defined, and characteristic to a particular isotope. It is for this reason that γ decays are often used to identify radioactive elements.

2.2.5 Decay Chains

Unstable nuclei can decay back to the valley of stability through the following processes:

- Alpha decay: ${}^A_Z\text{X} \longrightarrow {}^{A-4}_{Z-2}\text{Y} + {}^4_2\text{He}$
- Beta decay: ${}^A_Z\text{X} \longrightarrow {}^A_{Z+1}\text{Y} + e^- + \bar{\nu}_e$
- Positron emission: ${}^A_Z\text{X} \longrightarrow {}^A_{Z-1}\text{Y} + e^+ + \nu_e$
- Electron capture: ${}^A_Z\text{X} + e^- \longrightarrow {}^A_{Z-1}\text{Y} + \nu_e$

Which process an unstable nucleus actually undergoes depends on the values of A and Z.

It is clear from the above that any sequence of radioactive decays will only change the mass number A in units of four. This leads to the idea of decay chains, named after their starting isotopes, as follows:

	Name of chain	Starting isotope	Half-life of starting isotope (years)
$A = 4n$	Thorium	^{232}Th	1.41×10^{10}
$A = 4n+1$	Neptunium	^{237}Np	2.14×10^{6}
$A = 4n+2$	Radium	^{238}U	4.47×10^{9}
$A = 4n+3$	Actinium	^{235}U	7.04×10^{8}

There are actually no naturally occurring isotopes in the 'Neptunium' decay chain, as they have al decayed to stable elements due to the short lifetime of ^{237}Np in comparison to universal timescales.

2.3 Nuclear Fission and Fusion

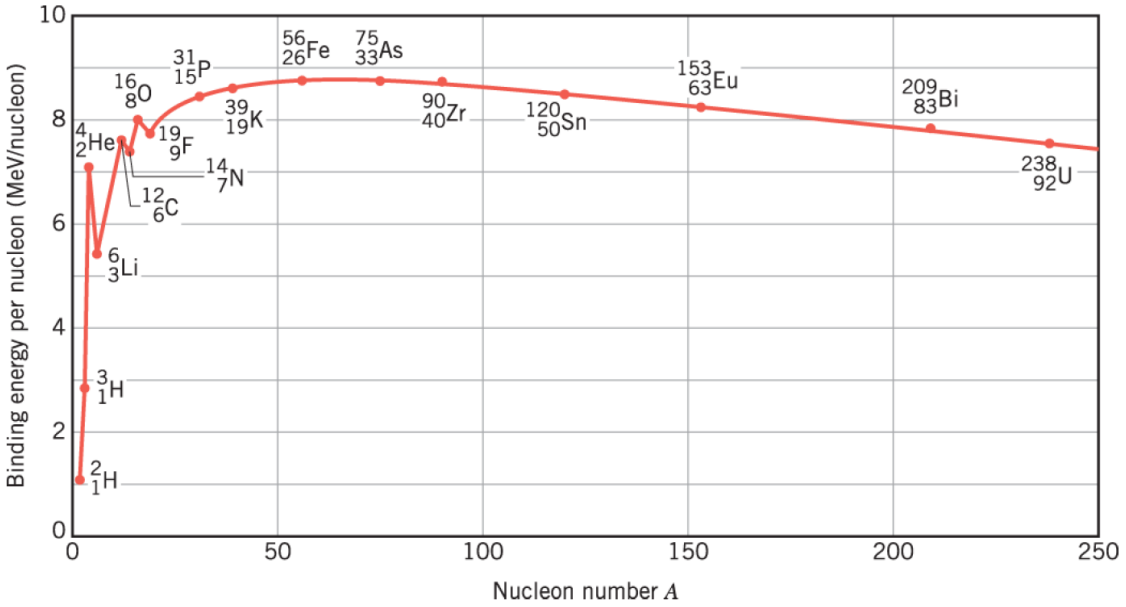

Figure 2.3: The binding energy per nucleon as a function of the mass number A

Consider figure 2.3 above. Given that it is energetically favourable for nuclei to maximise this binding energy, we can see that in the left-most region, *nuclear fusion* is prominent, while in the right-most region *nuclear fission* can occur. Both of these processes are distinct from the decays examined above as they involve the decay of the entire nucleus, rather than of individual protons or neutrons.

2.3.1 Fusion

Fusion is the process whereby two or more atomic nuclei come close enough to coalesce into a single nucleus. However, in order to do so, the two nuclei must overcome their mutual Coulomb repulsion. For example, consider the proton-proton (p-p) fusion process:

$$p + p \longrightarrow D + e^{+} + \nu_e \tag{2.44}$$

We can approximate the energy barrier by

$$E_{\text{barrer}} \approx \frac{\hbar c \alpha_{EM}}{2\,\text{fm}} \approx 0.7\,\text{MeV} \tag{2.45}$$

If each proton has energy of order $E_{\text{barrier}}/2$, the corresponding temperature is $\approx 4 \times 10^{9}\,K$, which is unusual even inside stars (here the fusion only occurs because of quantum tunnelling through the Coulomb barrier, and the high-energy tail of the Boltzmann velocity distribution).

In *tokamaks* (fusion reactors, of sorts), the reaction used is between deuterium (that can be extracted from sea water) and tritium (unstable $t_{1/2} \approx 12$ years, artificially produced) as follows:

$$^{2}_{1}\text{D} + ^{3}_{1}\text{T} \longrightarrow ^{4}\text{He} + n \tag{2.46}$$

This D-T reaction is used because it combines a large resonant cross section and a large Q value. The temperature inside typical tokamaks reaches $\approx 10^{8}\,K$, enough to produce at least some fission processes. The only - no so insignificant - problem is the containment of the reaction for an extended duration at these temperatures.

2.3.2 Fission

Fission is the splitting of a nucleus into two daughter nuclei. This occurs when the nucleus is massive enough that the barrier provided the the electrostatic interaction is small. We can model this process as the pulling apart of two charged spheres. During their separation, the charges move further apart, decreasing the magnitude of the Coulomb term in the SEMF (2.5). However, the surface area must increase, resulting in an increase in surface energy. We can thus approximate the barrier height at the point at which the daughter nuclei have *just* separated by

$$E_{\text{barrier}} = \frac{\text{Coulomb Energy}}{\text{Surface energy}} = \frac{\hbar c \alpha_{EM}(Z/2)^2}{2r_0(A/2)^{1/3}} \tag{2.47}$$

where $Z/2$ and $A/2$ are the atomic number and mass number respectively of the daughter nuclei (assumed symmetric split). For $A \approx 200$, the barrier is small enough that tunnelling can occur, the rate of which dictates the rate of *spontaneous fission.*

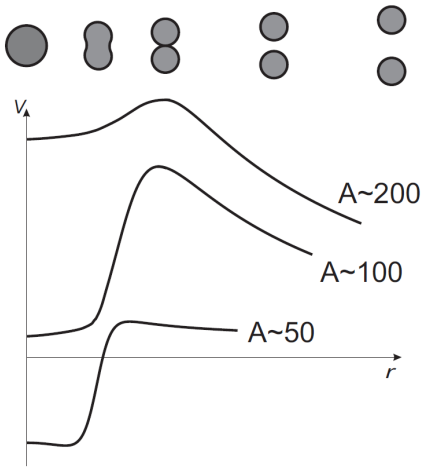

Figure 2.4: The shape of the potential barrier against fission for different values of the mass number A. Above, we have indicated a visual representation of their separation

However, we can also induce fission. Suppose that a thermal neutron ($\backsim$ eV) is incident on a nucleus with odd neutron number N. This will lead to an even N nucleus. This will liberate the normal binding energy, plus the energy from the δ pairing term as the even N state is lower in energy than the odd N state. For some elements, this liberates enough energy to give a large enough probability of tunnelling through the Coulomb barrier, and thus inducing fission. Apart from the energy liberated and the daughter nuclei, the fission also produces - on average - some extra neutrons. These may either be absorbed by non-fissile material, or go onto induce further fissions, leading to a chain reaction.

The canonical examples of fissile materials are the uranium isotopes ^{238}U and ^{235}U. ^{238}U does not undergo fission with thermal neutrons (only possible for $\backsim$ MeV neutrons), as bombardment with these neutrons leads to a γ decay process:

$$^{238}\text{U} + n \longrightarrow ^{238}\text{U}^* \longrightarrow ^{238}\text{U} + \gamma \tag{2.48}$$

However, ^{235}U is fissile as the transition from an even-odd nucleus ($^{235}_{92}$U) to an even-even nucleus ($^{236}_{92}$U) releases the pairing energy, allowing fission to occur:

$$^{235}\text{U} + n \longrightarrow ^{236}\text{U}^* \begin{cases} \xrightarrow{84\%} \text{Fission} \\ \xrightarrow{16\%} ^{236}\text{U} + \gamma \end{cases} \tag{2.49}$$

We can approximate the energy released in a ^{235}U fission process by considering an example. Suppose that such a uranium nucleus undergoes the process:

$$^{235}\mathrm{U} + n \longrightarrow ^{236}\mathrm{U}^* \longrightarrow ^{140}\mathrm{X} + ^{93}\mathrm{Y} + 3n + \gamma \tag{2.50}$$

The fission fragments are neutron rich, meaning that they must undergo beta decay to reach the valley of stability. In terms of the proton to neutron ratio, the daughter nuclei will lie close to some line passing through the origin of an N-Z plot and ^{235}U. We thus find that

$$\frac{N}{Z} \approx \frac{235 - 92}{92} \approx 1.55 \tag{2.51}$$

This allows us to approximate the daughter nuclei as ^{140}Kr and ^{93}Ba. Using (2.16), we can approximate that these daughter nuclei decay by beta decay (no change in A) into $^{140}_{58}$Ce and $^{93}_{41}$Nb. Then, the total energy released in the fission process is given by the difference in binding energy between the original ^{235}U nucleus and these decay products:

$$\frac{\Delta E}{c^2} = M(235, 92) - M(140, 58) - M(93, 41) - 2m_n \approx 200\,\mathrm{MeV} \tag{2.52}$$

This means that fission reactions with ^{235}U typically release in the region of 200 MeV, power that can be harnessed by appropriate containment of the reaction.

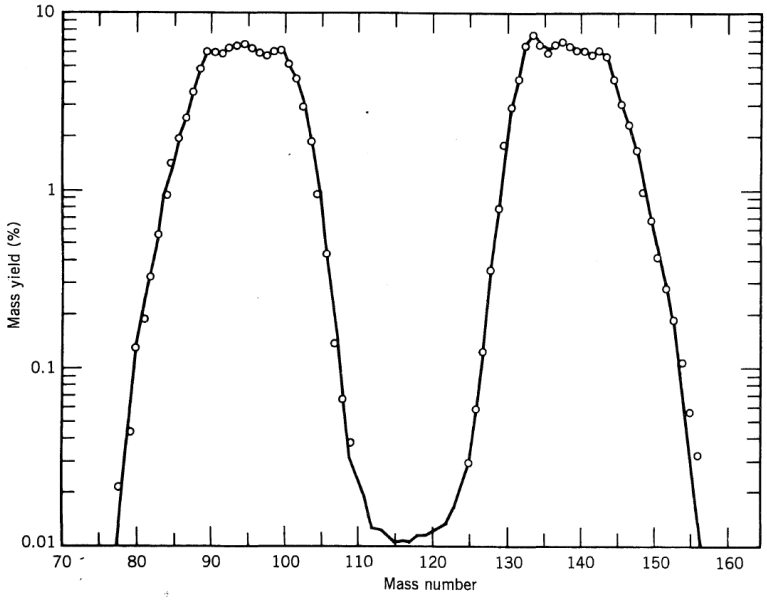

Figure 2.5: Mass distribution of the products from ^{235}U fission

Neutron Moderation

The neutrons produced in these reactions have very high energies, and have a high collision cross section for capture by ^{238}U in the enriched uranium fuel samples. In order to avoid this, *moderators* are used to slow the neutrons down to thermal speeds to prevent them being captured by ^{238}U nuclei before inducing another fission reaction, and so allowing the chain reaction to be sustained.

As a model of moderation, consider an elastic collision between a moving body of mass m with another, initially stationary, body of mass M. We can ignore electromagnetic effects as the neutron is uncharged. In the centre of momentum frame, let the speed of the first

mass be u, and that of the second be $U = um/M$, with associated scattering angle θ. In the lab, the speed of m before the collision is

$$v_{\text{in}} = u + U \tag{2.53}$$

whereas after the collision it is given by v_{out} where

$$v_{\text{out}}^2 = v_{\text{out}\parallel}^2 + v_{\text{out}\perp}^2 = (u\cos\theta + U)^2 + (u\sin\theta)^2 = u^2 + 2Uu\cos\theta + U^2 \tag{2.54}$$

The fraction of energy lost by m in the lab frame is $v_{\text{out}}^2/v_{\text{in}}^2$. To find the average energy loss, we need to average over the scattering angle θ. Assuming the scattering occurs isotropically, we have that

$$\langle\cos\theta\rangle = -\int_{-1}^{1} d(\cos\theta)\ \cos\theta = 0 \tag{2.55}$$

That is, there is no preferred scattering angle. The average fractional energy lost by m is given by

$$\left\langle \frac{E_{\text{out}}}{E_{\text{in}}} \right\rangle = \frac{u^2 + U^2}{(u+U)^2} = \frac{m^2 + M^2}{(m+M)^2} \tag{2.56}$$

The above expression has a minimim at $m \equiv m_n M$; the ideal moderator contains nuclei that have mass comparable to that of the neutron. This is why H_2O, D_2O and graphite are relatively suitable for this use. They also have a relatively low cross-section for electron capture. In the ideal case that the moderator has $A = 1$, half of the initial neutron energy will be lost on average per collision. An initial 1 MeV neutron will then cool to 0.1 eV after approximately $\log_2(\text{MeV}/0.1\,\text{eV}) \approx 23$ collisions.

Usually, lumps of fuel (rods) are embedded in a matrix of moderator material, rather than being completely mixed up with the moderator. This is because, since the mean free path of the fast electrons is less than the mean free path of the slow electrons ($\lambda_{\text{fast}} < \lambda_{\text{slow}}$), more of the fuel 'lump' can be seen by the thermal neutrons in this way. This would not be the case if the fuel and moderator were completely mixed up. It would also be very hard to extract power from the system if they were completely mixed together.

3. *Quarks and Hadrons*

This chapter aims to introduce the basic material underlying the Quark Model of hadrons, including

- Symmetries and Substructure
- Mesons
- Baryons
- The Quark Model

It is now time to migrate to sub-nuclear scales, and investigate the structure of matter itself. As we shall see, considerations of the symmetries of our system gives rise to the idea of quarks, which make up all strongly interacting matter. A useful numerical value to remember:

$$\hbar c \approx 197 \text{ MeV fm}$$

3.1 Symmetry and Substructure

The proton and the neutron have very similar masses and, despite one being charged and the other neutral, interact in the same way under the strong force. This suggests that the proton and the neutron might have some common internal structure, which can be invesigated by searching for similar patterns of multiplets of particles.

The lightest strongly interacting particles are the *pions*, which can be produced by firing protons ($\backsim$ GeV) into materials. Different pion creation reactions are observed:

$$\begin{aligned} p + p &\longrightarrow p + p + \pi^0 \\ p + p &\longrightarrow p + p + \pi^+ + \pi^- \\ p + n &\longrightarrow p + n + \pi^0 + \pi^+ + \pi^- \end{aligned} \tag{3.1}$$

There are three types of pions; the π^0, π^+ and π^- which have charges 0, +1 and -1 respectively. The latter two of which are antiparticles of one another. These have masses:

$$m_{\pi^0} = 135.0\,\mathrm{MeV}/c^2, \quad m_{\pi^\pm} = 139.6\,\mathrm{MeV}/c^2 \tag{3.2}$$

Another such group of particles are the delta baryons, that are created as resonances in reactions between pions and nucleons:

$$\begin{aligned} \pi^- + n &\longrightarrow \Delta^- \longrightarrow \pi^- + n \\ \pi^- + p &\longrightarrow \Delta^0 \longrightarrow \pi^0 + n \\ \pi^+ + n &\longrightarrow \Delta^+ \longrightarrow \pi^0 + p \\ \pi^+ + p &\longrightarrow \Delta^{++} \longrightarrow \pi^+ + p \end{aligned} \tag{3.3}$$

All of these delta baryons have a rest mass energy close to 1232 MeV, with spin quantum number $s = 3/2$. These decay in a very short time ($\backsim 10^{-22}$ s), and so cannot be observed as propagating particles; their mass is inferred from the width of the resonance peak using a version of the Breit-Wigner formula (1.79).

In the reactions involving the pions, we observe that the total number of protons and neutrons is conserved. This is a special case of *baryon number* conservation; protons and neutrons each have baryon number +1, while their anti-particles have baryon number −1. The second set of delta reactions also conserves baryon number, but protons and neutrons can be changed into one another due to the resonance. Baryon number conservation keeps the proton stable, since it forbids the decay of the proton into the lower mass pions. In fact, the lower bound for the lifetime of the proton is $\tau_p \gtrsim 1.6 \times 10^{25}$ years is much longer than the lifetime of the universe.

3.1.1 Isospin

Isospin was a concept proposed by Heisenberg in order to differentiate between the proton and the neutron; he posited that they are both states of the same entity, the nucleon, but with differing values of isospin components. The name 'isospin' is used in analogy to the spin, since the algebra of the isospin states have the same structure as the angular momentum states in quantum mechanics. However, isospin is completely separate from angular momentum; it is simply an internal quantum number of the system that tells us about quark content, as we shall see.

The quantum number I is the total isospin quantum number, while I_3 is the third component of the isospin, analogous to the m_j, m_ℓ and m_s for angular momentum. It is this latter component that differentiates between the proton and the neutron:

$$p = \left|\frac{1}{2}, \frac{1}{2}\right\rangle, \quad n = \left|\frac{1}{2}, -\frac{1}{2}\right\rangle \tag{3.4}$$

They thus form a nucleon doublet with $I = 1/2$ and $I_3 = \pm 1/2$. Similarly, we can write the isospin states of the pions and delta baryons:

$$\pi^+ = |1, 1\rangle, \quad \pi^0 = |1, 0\rangle, \quad \pi^- = |1, -1\rangle \tag{3.5}$$

$$\Delta^{++} = \left|\frac{3}{2}, \frac{3}{2}\right\rangle, \quad \Delta^{+} = \left|\frac{3}{2}, \frac{1}{2}\right\rangle, \quad \Delta^{0} = \left|\frac{3}{2}, -\frac{1}{2}\right\rangle, \quad \Delta^{-} = \left|\frac{3}{2}, -\frac{3}{2}\right\rangle \tag{3.6}$$

It is clear that there are $2I + 1$ states within a given isospin multiplet I. By analogy to angular momentum in quantum mechanics, we can also introduce the lowering and raising operators for isospin

$$I_\pm = I_1 \pm iI_2, \quad [I_i, I_j] = i\epsilon_{ijk} I_k \tag{3.7}$$

where I_1 and I_2 are the first and second components of the isospin. Applied to some state $|I, I_3\rangle$, these lower and raise the value of I_3 by one unit:

$$I_\pm |I, I_3\rangle = \sqrt{(I \mp I_3)(I \pm I_3 + 1)}\, |I, I_3 \pm 1\rangle \tag{3.8}$$

For example, $I_- \Delta^{++} = \sqrt{3}\Delta^+$ while $I_+ \Delta^{++} = 0$. We shall revisit these operators when we deal explicitly with quarks in later sections.

Invariance under rotation in isospin space implies the conservation of isospin in nuclear interactions, meaning that the strong force preserves isospin. We can use this to calculate the relative magnitudes of cross sections and branching ratios in strong interactions, as in the following example.

The cross section for the reaction $\pi^- p \longrightarrow \pi^0 n$ shows a prominent peak when measured as a function of the π^- energy. The peak corresponds to a Δ baryon resonance of 1232 MeV, with total width $\Gamma = 120$ MeV. The find the ratio of the incoming and outgoing partial widths Γ_i and Γ_f.

From above, the intermediate state is given by

$$|\Delta\rangle = \left|\frac{3}{2}, I_3^\Delta\right\rangle \tag{3.9}$$

However, as I_3 must be conserved in strong interactions, we have that

$$I_3^\Delta = I_3^{\pi^0 n} = -\frac{1}{2} \quad \longrightarrow \quad |\Delta\rangle = |\Delta^0\rangle = \left|\frac{3}{2}, -\frac{1}{2}\right\rangle \tag{3.10}$$

As in quantum mechanics, we can expand this state in terms of the Clebsh-Gordan coefficients c_{ab}

$$\left|I^a, I^b, I^\Delta, I_3^\Delta\right\rangle = \sum_{a,b} c_{ab} \left|I^a, I^b, I_3^a, I_3^b\right\rangle \tag{3.11}$$

for two particles a and b. For the protons and neutrons, $I^a = 1/2$, while for the pions $I^b = 1$. We can thus write that

$$|\Delta^0\rangle = \left|\frac{1}{2}, 1, \frac{3}{2}, -\frac{1}{2}\right\rangle = \sqrt{\frac{2}{3}}\left|\frac{1}{2}, 1, 0, -\frac{1}{2}\right\rangle + \sqrt{\frac{1}{3}}\left|\frac{1}{2}, 1, -1, \frac{1}{2}\right\rangle = \sqrt{\frac{2}{3}}\,|\pi^0 n\rangle + \sqrt{\frac{1}{3}}\,|\pi^- p\rangle \tag{3.12}$$

The ratio of the incoming to the outgoing partial widths is thus

$$\frac{\Gamma_i}{\Gamma_f} = \frac{\left|\langle \Delta^0 | \pi^- p \rangle\right|^2}{|\langle \Delta^0 | \pi^0 n \rangle|^2} = \frac{1/3}{2/3} = \frac{1}{2} \tag{3.13}$$

Conservation of isospin is a powerful tool that we will make further use of later on in this text.

3.1.2 Symmetries

Before delving further into this subatomic world, let us pause to consider possible symmetries of our system. A symmetry is a physical or mathematical feature of the system that is preserved or remains unchanged under some transformation. This transformation may be continuous (such as a rotation) or discrete (such as a reflection). In the case of continuous transformations, there give rise to cyclic coordinates, and a corresponding conserved quantity. For example, translational invariance implies momentum conservation, while rotational invariance implies angular momentum conservation. We shall examine some symmetries relevant to our study of subatomic particles.

Parity

A *parity inversion* $\mathcal{P}$ is a transformation involving the reversal of the sign of one spatial coordinate. In three dimensions, it describes a simultaneous switch of all of the coordinates (a point inversion):

$$\mathcal{P} : \mathbf{x} \mapsto -\mathbf{x} \tag{3.14}$$

We can classify vectors based on the way that they transform under a parity inversion:

- Polar - These reverse their sign under parity inversion (eigenvalue -1)
- Axial - These do not reverse their sign under parity inversion, often associated with cross-product type quantities (eigenvalue $+1$)

A *pseudoscalar* (such as a triple product) is a quantity that behaves like a scalar, except that it changes sign under parity inversion. Fermions and anti-fermions have opposite parity, and by conventions, fermions are assigned positive parity.

We know that for a single particle in a state of well-defined orbital angular momentum, applying a parity inversion to the state has the following effect:

$$\mathcal{P} |n, \ell, m_\ell\rangle = (-1)^\ell |n, \ell, m_\ell\rangle \tag{3.15}$$

The parity of the combined state of two particles must then be the product of the parities of the individual particles, and an extra factor from treating the two particles as a combined system. We can thus write that

$$\boxed{P_{ab} = P_a P_b (-1)^L} \tag{3.16}$$

where L is the total orbital angular momentum of the two particle system around the centre of mass, and P_{ab}, P_a, P_b are the parity eigenvalues of the combined state and the individual particles respectively.

Both the strong and electromagnetic interactions conserve parity. However, the weak interaction does not; not only does it not, but it violates parity conservation maximally. This can be tested by looking at the following beta decay process:

$$^{60}\mathrm{Co} \longrightarrow ^{60}\mathrm{Ni} + e^- + \bar{\nu}_e \tag{3.17}$$

The Co is cooled to 0.01 K, and immersed in a strong magnetic field $\mathbf{B}$ so that the nuclear spins are preferentially aligned along the magnetic field. The directions of the outgoing beta electrons are then observed. Consider the behaviour of the momentum vector $\mathbf{p}$ of the observed electrons, and the magnetic moment direction $\boldsymbol{\mu}$ of the nuclei under parity inversion:

$$\mathcal{P} : \mathbf{p} \mapsto -\mathbf{p}, \quad \mathcal{P} : \boldsymbol{\mu} \mapsto \boldsymbol{\mu} \tag{3.18}$$

After a parity inversion, the momentum vector in inverted, but the nuclear spin points in the same direction. Therefore if parity is to be conserved, there must be as many electrons emitted in the $+\mathbf{B}$ direction as in the $-\mathbf{B}$ direction. However, it was observed that the emission of electrons was not symmetric with respect to the magnetic field direction. This means that while the initial cobalt nucleus was in a state of well-defined parity, the final state is not. Thus, the Hamiltonian of the system is not parity invariant. As the Hamiltonian encodes the weak interaction responsible for this decay, we are then also forced to conclude that the weak interaction violates parity conservation.

Charge Conjugation

The *charge conjugation* transformation replaces particles with anti-particles. Suppose that a represents some particle, and $\bar{a}$ represents the corresponding antiparticle. Then, the charge conjugation operator $\mathcal{C}$ has the action:

$$\mathcal{C} : a \mapsto \bar{a} \tag{3.19}$$

Only neutral particles have the possibility of being eigenstates of $\mathcal{C}$ as turning a particle into an anti-particle involves changing the sign of the charge value. Applying $\mathcal{C}$ twice must return the system to its original state, and so the possible eigenvalues for charge conjugation are ± 1. In fact, for a system of angular momentum quantum numbers J, L and S, we have that

$$\mathcal{C} \left| a, \bar{a}, J, L, S \right\rangle = (-1)^{L+S} \left| a, \bar{a}, J, L, S \right\rangle \tag{3.20}$$

for both fermions and bosons (recalling exchange symmetries). As with parity, charge conjugation is a symmetry of the electromagnetic and strong interactions, but not the weak interaction. As a result of the consequences of parity and charge conjugation on conserved quantities, it is often useful to notate particles as

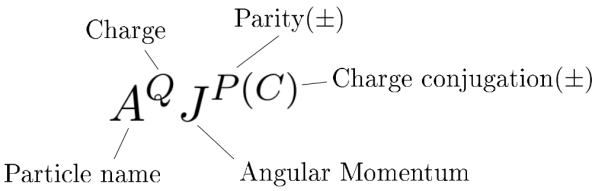

Figure 3.1: The conventional notation used to refer to subatomic particles

Time Reversal

Time reversal symmetry implies invariance under the transformation $t \mapsto -t$, leaving all positions in the system unchanged. There is no physical observation that belongs to the time reversal operator, so there is no observable which would be conserved. However, there is a very fundamental theorem in QFT, which states that 'any Lorentz-invariant local quantum field theory with a hermitian Hamiltonian must have symmetry under a combined CPT operation'. As a consequence, we assume that time reversal symmetry is also violated in weak processes (such that CPT symmetry is satisfied), which is borne out in experiments.

3.2 Mesons

Isospin symmetry implies that there is some substructure to all of these particles that we have examined; just like the nuclei of isotopes of elements contain a particular combination of protons and neutrons (to give a specific Z and A), there must be some smaller particle that interacts via the strong force to form these particles with specific values of I and I_3. These particles are known as *quarks*, and the particles that they combine to form are known as *hadrons*. Quarks are spin-half particles, meaning that they obey Fermi-Dirac statistics.

Mesons are hadrons fromed from a quark and an anti-quark pair, $q\bar{q}$, and have integer spins. As the parity of the quark is set to be positive ($P = 1$) by convention, the anti-quark must have negative parity ($P = -1$). The parity state of a meson in a state of well-defined orbital angular momentum L is

$$\boxed{P_{\text{meson}} = (-1)^{L+1}} \tag{3.21}$$

The pions introduced in section 3.1 are in fact mesons. They are composed of two different quarks, the *up* and *down*, which have the following properties:

Name	Flavour	Mass (GeV/c^2)	$Q(e)$	I	I_3	S	B	J
Up	u	0.002	2/3	1/2	1/2	0	1/3	1/2
Down	d	0.005	-1/3	1/2	-1/2	0	1/3	1/2

The *flavour* of a quark is the specific type of quark that is involved i.e whether it is an up or down quark. Antiquarks have the opposite sign of Q, I_3, S and B. Using these properties, it becomes clear that the nucleons and pions are written as

	Quarks	Mass (MeV/c^2)	$Q(e)$	I	I_3	S	B	J
π^+	$u\bar{d}$	139.6	1	1	1	0	0	0
π^0	$u\bar{u}, d\bar{d}$	135.0	0	1	0	0	0	0
π^-	$d\bar{u}$	139.6	-1	1	-1	0	0	0

Note that these are all spin-0 particles due to fact that the spins of the quark and anti-quark are anti-aligned. We have started to construct our particle zoo.

3.2.1 Strangeness

If we raise the energy of our scattering experiments, we begin to find particles with a mass of $\approx 500\,\text{MeV}/c^2$ with integer spin (mesons) and $\approx 1200\,\text{MeV}/c^2$ with half-integer spins (which turn out to be baryons, see section 3.3). These particles appear to satisfy all the conservations that are associated with strong processes, but they decay on timescales of weak decays ($\backsim 10^{-12}$ s). We thus propose the existence of a property called *strangeness* S that is conserved in strong interactions, but violated in weak interactions. These newly observed particles would have $S \neq 0$. As such, we introduce a third *strange* quark:

Name	Flavour	Mass (GeV/c^2)	$Q(e)$	I	I_3	S	B	J
Strange	s	0.095	-1/3	0	0	-1	1/3	1/2

The lightest strange mesons are the kaons K^+, K^-, K^0 and $\bar{K}^0$ (note that the K^0 is distinct from its antiparticle as can undergo different reactions with matter). Their exact quark content is detailed in the following section.

3.2.2 Meson Multiplets

With three quarks, there are thus $3 \otimes 3 = 9$ combinations that we can make. This means that we can organise our mesons into sets of nine (nonets) that are differentiated by their differing values of J and P. In particular, we consider the $J^P = 0^-$ nonet

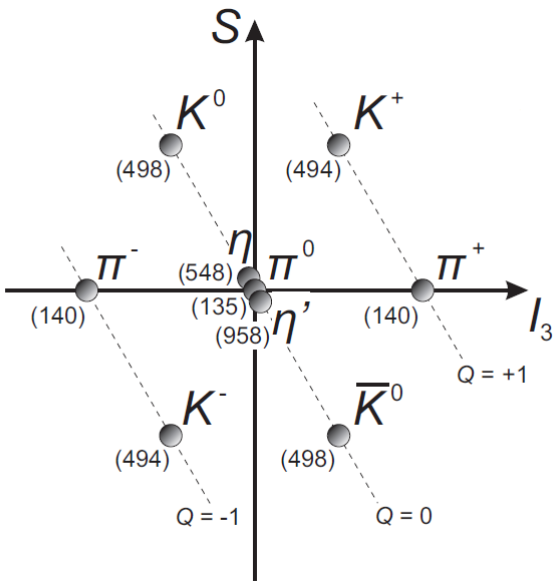

Figure 3.2: The $J^P = 0^-$ nonet. All masses are in units of MeV/c^2

Six of these decay weakly ($\backsim 10^{-10}$ s), while three decay electromagnetically (π^0, η and η'). We also have the $J^P = 1^-$ (note that in this case, $L = 0$, so $J = S = 1$ with the quarks aligned) nonet:

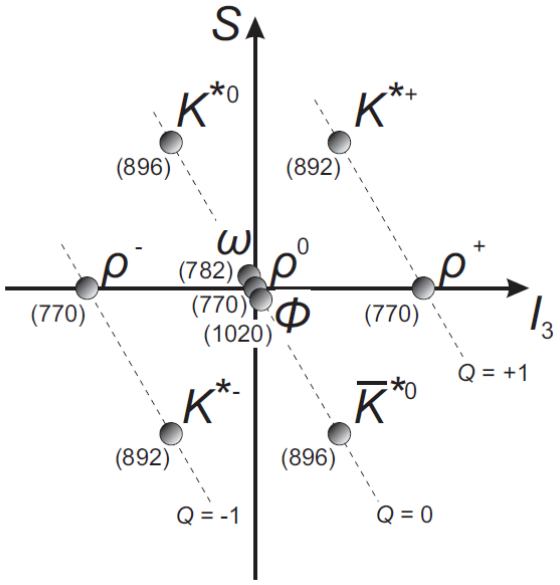

Figure 3.3: The $J^P = 1^-$ nonet. All masses are in units of MeV/c^2

These mesons have much shorter lifetimes (strong, $\backsim 10^{-24}$ s), decaying into the $J^P = 0^-$ mesons.

Both the $J^P = 0^-$ and $J^P = 1^-$ mesons have exactly the same quark composition, but they differ by a factor of order unit in mass. This allows us to conclude that the dominant contribution to the meson mass comes from the interaction between the quarks, particularly the spin dependence.

3.2.3 Quark Flow Diagrams

A quark flow diagram is a useful way to visualise collision reactions at the level of quarks. As an example, let us again consider the process:

$$\begin{array}{ccccccc} \pi^- + & p & \longrightarrow & \Delta^0 & \longrightarrow & \pi^0 + & n \\ d\bar{u} + & uud & \longrightarrow & udd & \longrightarrow & d\bar{d} + & udd \end{array} \tag{3.22}$$

We have written the quark content explicitly in the second line (for the quark content of the proton and neutron, see section 3.3). In the first part of the reaction, a $\bar{u}$ in the pion annihilates against a u in the proton, leaving the udd state that corresponds to the Δ^0. In the decay, a quark-antiquark pair is created to form a neutral pion and neutron. This is shown in figure 3.4 below.

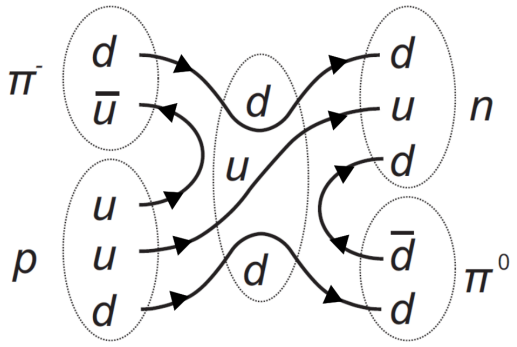

Figure 3.4: An example of a quark flow diagram for the $\pi^- p \longrightarrow \Delta^0 \longrightarrow \pi^0 + n$ process

This also allows us to understand why the K^0 and $\bar{K}^0$ will behave differently on interaction with matter. $\bar{K}^0$ is able to form a uds resonance with neutrons (udd), where as K^0 cannot.

Lastly, quarks can only annihilate against antiquarks of the same flavour, quark flavour is conserved throughout all strong interactions. This is a characteristic property of strong interactions.

3.3 Baryons

Baryons are hadrons made from a combination of three quarks, and have half-integer spins. We can calculate the parity of the baryon states by remarking that the spin will be $\frac{1}{2} \otimes \frac{1}{2} \otimes \frac{1}{2}$, which is either $\frac{1}{2}$ or $\frac{3}{2}$. The parity of a baryon is a state of well defined orbital angular momentum L is thus

$$\boxed{P_{\text{baryon}} = (-1)^L} \tag{3.23}$$

For the lowest energy (lightest) $L = 0$ states, the parity is positive, meaning that we expect to have the states $J^P = \frac{1}{2}^+$ and $J^P = \frac{3}{2}^+$. For $J^P = \frac{1}{2}^+$, we find eight particles of similar mass, giving the octet below. Particles in this octet are either stable (proton)

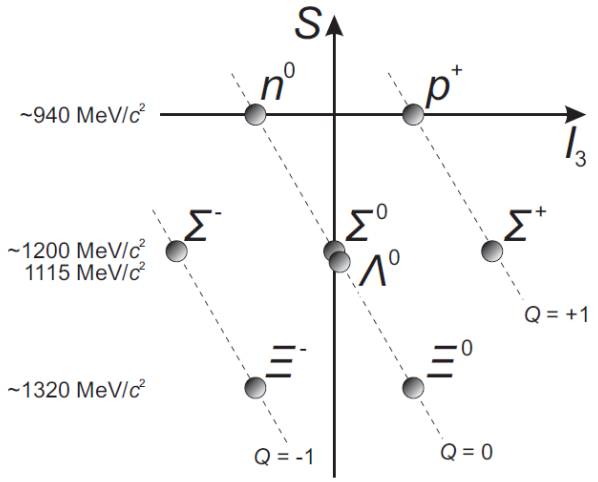

Figure 3.5: The $J^P = \frac{1}{2}^+$ octet

or decay on timescales that are comparable to weak decays (except for Σ^0 which decays electromagnetically: $\Sigma^0 \longrightarrow \Lambda^0 + \gamma$). For $J^P = \frac{3}{2}^+$ there are ten particles:

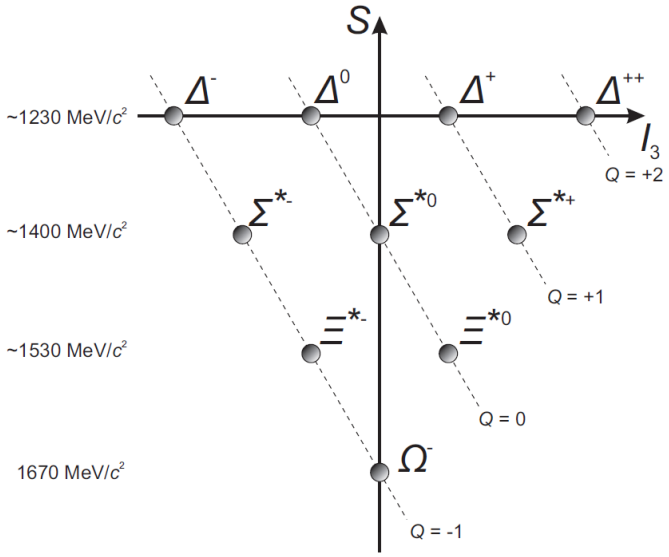

Figure 3.6: The $J^P = \frac{3}{2}^+$ decuplet

These decay strongly to a $J^P = \frac{1}{2}^+$ baryons, with the exception of the Ω^-, which can only decay weakly as the strangeness must change.

3.3.1 Quark Colour

It is thus clear that under the quark model, the isospin symmetry is expanded into a more general quark *flavour symmetry*. However, there is some cause for concern. Baryons can be constructed as a combination of three quarks, so we have in principle $3 \otimes 3 \otimes 3$ combinations. How did we arrive at the 18 combinations in the $J^P = \frac{1}{2}^+, \frac{3}{2}^+$ states?

Consider the $J^P = \frac{3}{2}^+$ baryons with quark combinations *sss*, *uuu* and *ddd*. As these are fermions (spin-half) particles, and so we would expect them to behave appropriately under exchange symmetry. Consider the product state

$$|\psi\rangle = |\psi_{\text{spatial}}\rangle \times |\psi_{\text{flavour}}\rangle \times |\psi_{\text{spin}}\rangle \tag{3.24}$$

In the groundstate, the spatial state is symmetric. The flavour state is

$$|\psi_{\text{flavour}}\rangle = |u_1\rangle\,|u_2\rangle\,|u_3\rangle \tag{3.25}$$

which is clearly symmetric under the exchange of two quarks. Similarly, the spin state of these combinations must also be symmetric under exchange. This means that an overall state of the form (3.24) is symmetric under quark exchange, which it really should not be. We instead propose the state

$$|\psi_{\text{baryon}}\rangle = |\psi_{\text{spatial}}\rangle \times |\psi_{\text{flavour}}\rangle \times |\psi_{\text{spin}}\rangle \times |\psi_{\text{colour}}\rangle \tag{3.26}$$

where

$$|\psi_{\text{colour}}\rangle = \frac{1}{\sqrt{6}} \left|\left| \begin{pmatrix} r_1 & g_1 & b_1 \\ r_2 & g_2 & b_1 \\ r_3 & g_3 & b_3 \end{pmatrix} \right|\right| \tag{3.27}$$

Note that || indicates the anti-symmetrised Slater determinant, ensuring that the overall wavefunction behaves appropriately upon particle exchange. This is also the only combination of the three colours red (r), green (g) and blue (b) that has no net colour. Quarks carry colour, while anti-quarks carry anti-colour. The colour in the mesons is contained in $q\bar{q}$ combinations in the superposition

$$|\psi^{\text{meson}}_{\text{colour}}\rangle = \frac{1}{\sqrt{3}}(|r\bar{r}\rangle + |g\bar{g}\rangle + |b\bar{b}\rangle) \tag{3.28}$$

which is also colourless. This is important, as the strongly interacting particles that we have observed all have no net colour; no coloured object (quark) has ever been observed in isolation. If - for example - we attempt to knock a u quark out of a proton, we do not observe a free u in the final state of the system; instead the u uses part of its kinetic energy to create other $q\bar{q}$ pairs, such that the final state only contains colour neutral hadrons.

The particles that carry the strong force between quarks are the *gluons*. Each gluon carries both a colour and an anti-colour. There are eight gluons, since of the nine possible distinct colour-anticolour combinations, one is colourless. We shall examine the properties of gluons more closely in section 4.2.

Evidence for Quark Colour

Experimental evidence for quark colour comes from looking at high energy electron-positron collisions. In particular, we can compare the collision cross sections for the processes:

$$e^+ + e^- \longrightarrow \mu^+ + \mu^-$$
$$e^+ + e^- \longrightarrow \text{hadrons}$$

Feynman diagrams for these processes are shown in figures (1.7) and (1.8) respectively. As both processes are assumed to have the same initial energy upon the e^+e^- annihilation, they have the same propagator factor. The vertex couplings are all electromagnetic, meaning that the only thing that is different between the two processes is the magnitude of the vertex factor; for the muons, the vertex factor is $(\pm 1)g_{\text{EM}}$, while for the decay into quarks (hadrons) it is $(\pm Q_q)g_{\text{EM}}$ (Q_q are the charges of the quarks relative to the proton). The density of states factors will be approximately the same if both processes occur at relativistic energies.

The ratio between the cross-sections for these two processes can thus be written as

$$R = \frac{\sigma(e^+e^- \longrightarrow \text{hadrons})}{\sigma(e^+e^- \longrightarrow \quad \mu^+\mu^-)} = \frac{3 \times g_{\text{EM}}^2 \sum_i Q_i^2}{1 \times g_{\text{EM}}^2} = 3\sum_i Q_i^2 \tag{3.29}$$

where the sum is over all the available $q\bar{q}$ states at a given centre of mass energy. We have included a factor of three for the decay into hadrons to take into account the possible colour combinations. Data from such experiments is shown in figure 3.7 below.

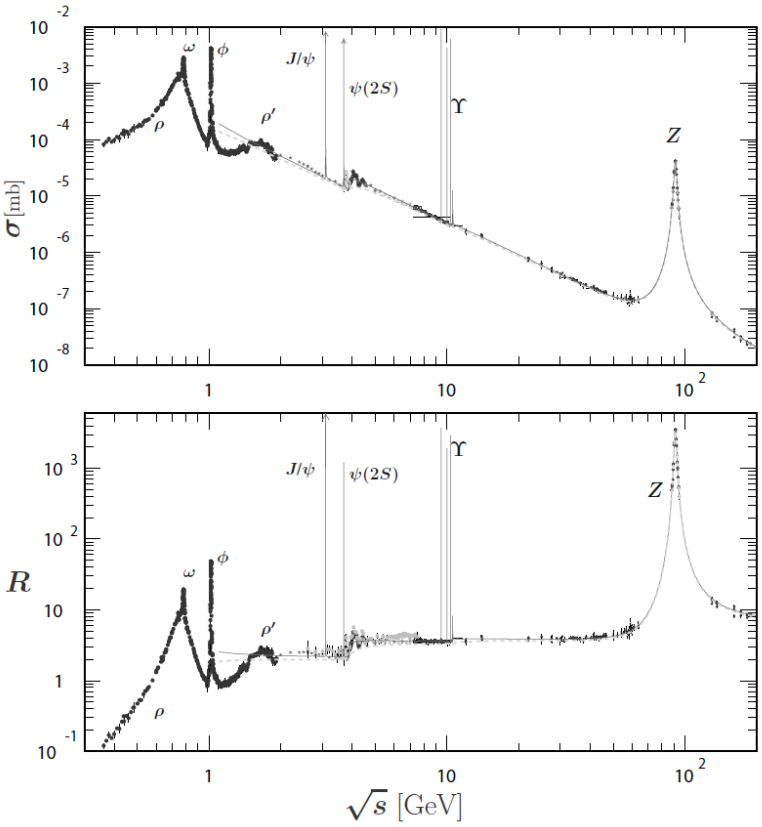

Figure 3.7: Data on the total cross section of $\sigma(e^+e^- \longrightarrow \text{hadrons})$ and R as a function of the centre of mass energy $\sqrt{s}$

From the second graph, it is clear that R has a number of values depending on the particular energy range:

(i) ≈ 2 GeV to ≈ 5 GeV: $R = 2$

(ii) ≈ 5 GeV to ≈ 10 GeV: $R = \frac{10}{3}$

(iii) ≈ 10 GeV to ≈ 20 GeV: $R = \frac{11}{3}$

Each of these regions corresponds to the presence of different amounts of quarks. In (i), only the u, d, s quarks are present, and the value of R appears to include the degrees of freedom for quark colour. The steps (ii) and (iii) correspond to the creation of more massive quarks, called the charm c and bottom b quarks respectively. There is also a sixth quark the top t, but this is too massive to be produced in e^+e^- collisions due to radiative losses. The top quark decays weakly (into a bottom quark, and either an $\ell\nu$ or $q\bar{q}$ pair), but due to its large mass, it decays faster than it can hadronise. As a consequence, there are no bound states containing top quarks.

The values of R correspond to these new quarks having a charge of $2/3$, $-1/3$ and $2/3$ respectively, which is indeed the case. We thus have three generations of quarks, each containing a $2/3$ and $-1/3$ partner:

$Q = 2/3$	u	c	t
$Q = -1/3$	d	s	b

(3.30)

The sharp resonance peaks at 3, 10 and 100 GeV are the bound charmonium $(c\bar{c}, \psi)$, bottomonium $(b\bar{b}, \Upsilon)$, and Z boson states. The latter has a broader peak than the others as they live longer before decaying. We shall discuss these bound states in later sections. The two sharp resonance peaks at 0.8 and 1 GeV correspond to ω and ϕ meson production respectively.

3.4 The Quark Model

Hadrons are subatomic particles that are mediated by the strong interaction. All hadrons are made up of some combination of the six quarks q:

Name	Flavour	Mass (GeV/c^2)	$Q(e)$	I	I_3	S	B	J
Up	u	0.002	2/3	1/2	1/2	0	1/3	1/2
Down	d	0.005	-1/3	1/2	-1/2	0	1/3	1/2
Charm	c	1.3	2/3	0	0	0	1/3	1/2
Strange	s	0.095	-1/3	0	0	-1	1/3	1/2
Top	t	174	2/3	0	0	0	1/3	1/2
Bottom	b	4.2	-1/3	0	0	0	1/3	1/2

where I = total isospin, I_3 = third component of isospin, S = strangeness, B = baryon number and J = total angular momentum. The charge of hadrons is related to the baryon number and third component of isospin by

$$Q = e\left(I_3 + \frac{1}{2}Y\right), \quad Y = S + C + B' + T + B \tag{3.31}$$

The quark model has the following further properties.

- Quarks come in three strong-charges, r, g, b known as colours
- Antiquarks $\bar{q}$ have the opposite values of all flavour quantum numbers except for J, and the mass is unchanged
- Quarks interact via the strong force, which conserves isospin. They are confined in the colourless combinations that are hadrons
- Mesons are colourless $q\bar{q}$ combinations
- Baryons are colourless qqq combinations
- Only weak interactions can change quark flavour

Together with the leptons, gauge bosons and the Higgs boson, the quarks make up the Standard Model of matter.

3.4.1 Quarkonium

In the previous section, we saw sharp resonance peaks that correspond to a bound $q\bar{q}$ system that is dominated by the masses of the constituents. In this case, the system can be reasonably well-described by non-relativistic quantum mechanics, for which the Time-Independent Schrödinger equation reads

$$\left(\frac{\mathbf{p}^2}{2\mu} + V\right)|\psi\rangle = E\,|\psi\rangle \tag{3.32}$$

where μ is the reduced mass of the $q\bar{q}$ system. The potential V due to the strong force between a quark and its antiquark partner is well described by the potential

$$\boxed{V(r) = -\frac{4}{3}\frac{\hbar c\alpha_s}{r} + kr} \tag{3.33}$$

The first term s the strong force equivalent of the Coulomb potential. We have replaced α_{EM} with $(4/3)\alpha_S$, where the factor of 4/3 comes from colour considerations. The term linear in r means that V continues growing as $r \to \infty$, leading to quark confinement.

In the case of the $c\bar{c}$ *charmonium* and $b\bar{b}$ *bottomonium* states, the typical separation r is usually smaller than $r_0 = 1/\sqrt{k}$, meaning that we can ignore the linear term. Under these conditions, the energy levels of these bound states can be approximated as hydrogenic:

$$E_n = -\frac{1}{2}\mu\left(\frac{4}{3}\alpha_S c\right)^2 \frac{1}{n^2} \tag{3.34}$$

The total energy of the $q\bar{q}$ states is thus given by

$$E_{q\bar{q}} = E_n + 2m_q c^2 \tag{3.35}$$

Charmonium

Let us consider the particular case of charmonium. Some of the lowest lying energy states are:

Name	$n^{2S+1}L_J$	J^P
η_c	1^1S_0	0^-
J/ψ	1^3S_1	1^-
h_c	1^1L_1	1^+
ψ'	2^3S_1	1^-

The first of these states that was discovered was the J/ψ state. This is because this state has $S = 1$, $L = 0$, such that $J^P = 1^-$, which has the same symmetries as the photon; it can thus be created in electron-positron collisions via an intermediate photon:

$$e^+ + e^- \longrightarrow \gamma^* \longrightarrow J/\psi \tag{3.36}$$

Measurement of these gamma-ray photon energies allows us to make a precise measurement of the mass differences between the energy levels, and thus the predictions of (3.34).

Charmonium has a few possible decay paths, as follows:

- Charmonium states may decay into the D mesons if they are sufficiently massive ($> 2m_D$, $m_D \approx 1865$ MeV/c^2). This decay is via the strong force into either a D^0 ($c\bar{u}$), $\bar{D}^0$, or a D^+ ($c\bar{d}$) and D^- ($\bar{c}d$) pair
- If the state is not massive enough for D meson decays, the system may also decay through the annihilation of the charm and anticharm quark. One way to do this is through an electromagnetic interaction, which produces a photon and subsequently another $q\bar{q}$ pair
- Another way to do this is via a suppressed version of the strong interaction. In this case, the resulting state does not contain any charm quarks, and so the intermediate state must consist of only gluons. This leads to what is known as 'OZI suppression', where the poor momentum coupling of the gluons causes a very large reduction in the decay rate. The decay is usually into into π^+, π^0 and π^-

This means that generally $c\bar{c}$ states with $m < 2m_D$ are long-lived, and are visible as very narrow resonances with masses close to 3 GeV.

The Strong Coupling Constant

Now, what is the value of the coupling constant for the strong force? We can estimate this using experimental data. If the splitting between the $n = 2$ and $n = 1$ states in the J/ψ $c\bar{c}$ system is 588 MeV, and $m_c = 1870$ MeV$/c^2$, it is straightforward to use (3.34) to calculate that $\alpha_S \approx 0.97$. Similarly, if the splitting between the $n = 2$ and $n = 1$ states in the Υ $b\bar{b}$ system is 563 MeV, and $m_b = 5280$ MeV$/c^2$, we find that $\alpha_S \approx 0.57$.

This means that, unlike α_{EM} the value of the strong force coupling constant scales with the momentum transfer q. More specifically, α_S is smaller for large q, and larger for smaller q (the bottomonium case has a higher mass with comparable energy, and so a higher momentum transfer). This also contributes to OZI suppression. However, for most calculations, one takes the value

$$\boxed{\alpha_S \approx 1} \tag{3.37}$$

This much larger value of α_S compared with the electromagnetic fine structure constant $\alpha_{\text{EM}} \approx 1/137$ is a reflection of the relative strength of the two forces.

3.4.2 Hadron Decays

As anticipated by our discussion of Charmonium, hadrons may decay via either the strong, electromagnetic or weak forces:

- Strong decays (rapid, $\tau \backsim 10^{-22}$ s) - The strong interaction allows reactions and decays in which quarks are interchanged between hadrons, but there is no change in net quark flavour; they conserve net quark content
- Electromagnetic decays (intermediate, $\tau \backsim 10^{-18}$ s) - Electromagnetic decays typically have lifetimes between those corresponding to strong and weak decays, and do not change quark flavour
- Weak decays (slow, $\tau \backsim 10^{-10}$ s) - If overall quark flavour is indeed changed, such as in the strangeness violating reactions

  $$\underset{u\bar{s}}{K^+} \longrightarrow \underset{ud}{\pi^+} + \underset{u\bar{u},d\bar{d}}{\pi^0} \qquad [\Delta S = -1]$$
  $$\underset{dds}{\Sigma^-} \longrightarrow \underset{udd}{n} + \underset{ud}{\pi^-} \qquad [\Delta S = +1]$$

  a weak interaction must be involved. This means that only weak interactions can change quark flavour. Weak decays are suppressed by factors of G_F in the transition matrix element $\mathcal{M}_{if}$, meaning that weakly decaying particles are characterised by quite long lifetimes

In general, decays (and reactions) are dominated by a particular mode. In general, we can apply the following rules to find the dominant mode of a reaction or decay:

1. A reaction or decay is dominated by the strongest interaction that is common to all participants. The interactions are ordered as Strong > Electromagnetic > Weak
2. If a photon is present in a reaction, then the strong interaction cannot dominate, meaning that the dominant interaction is either electromagnetic or weak
3. If a neutrino is present, then either neither the strong no electromagnetic interactions can dominate. The dominant interaction is then the weak interaction

The ordering of the strength of the forces may seem a little odd, given the relative magnitudes of the coupling constants ($\alpha_S > \alpha_W > \alpha_{\text{EM}}$). However, the weak interaction is.....well, weaker than the electromagnetic interaction on the scale of the quarks by a factor of $\backsim 10^{-6}$.

4. *The Standard Model*

In this section, we cover the main concepts associated with the Standard Model of matter, including:

- A Summary of the Standard Model
- The Strong Interaction
- The Weak Interaction
- Neutrino Oscillations

The time has finally come to tackle one of the crowning achievements of 21^{st} century physics; the Standard Model of matter. Students may already be familiar with the approximate structure of the Standard Model from even secondary school physics, but now we are able to motivate this structure on a much more fundamental level, as well as investigate some of its consequences.

4.1 A Summary of The Standard Model

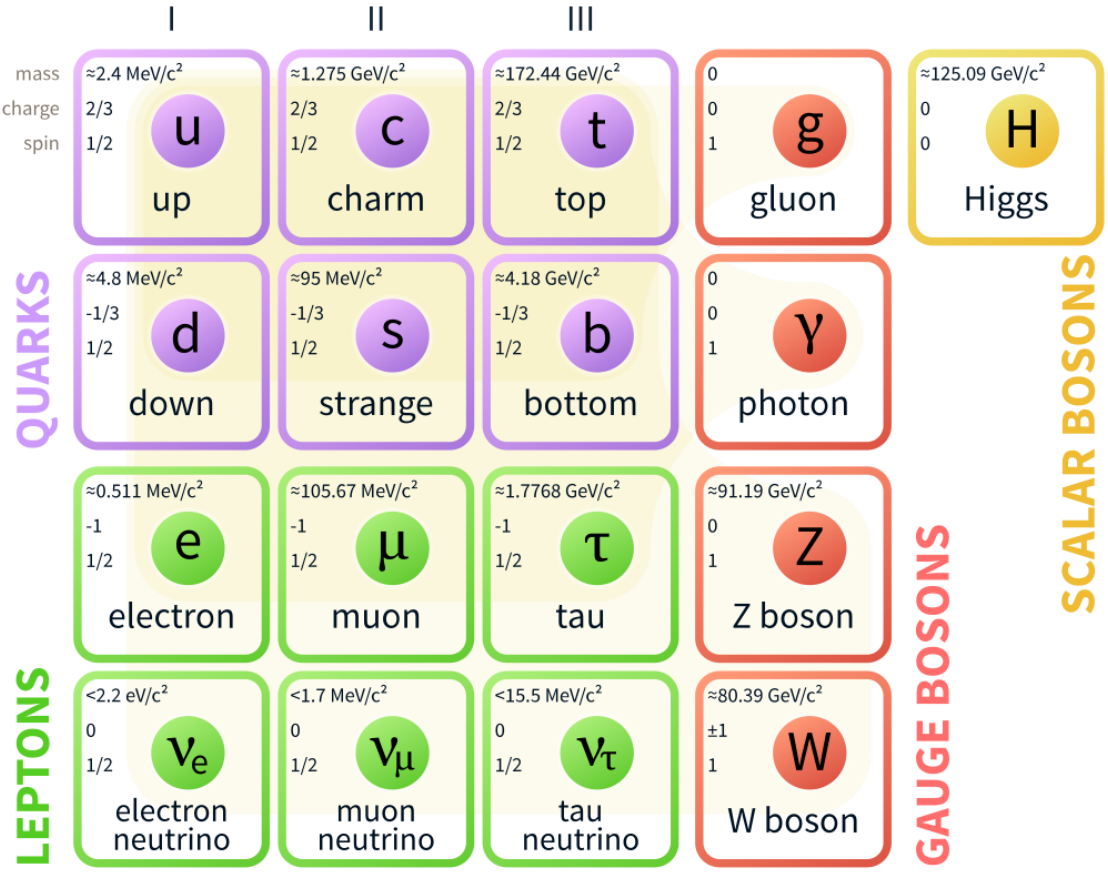

Figure 4.1: The canonical diagram for the Standard Model of Matter

The Standard Model, as it currently stands, consists of three main groups of particles. The spin-half quarks (u, d, c, s, t, b) make up all hadrons (mesons and baryons), matter particles that can undergo processes involving the strong interaction. The leptons (ℓ) are elementary spin-half particles that do not undergo processes involving the strong interaction. Mediating these interactions are the spin-one gauge bosons corresponding to the three (four) fundamental forces:

Force	Quantum	Mass[a]	Spin	Range	α	Strength[b]
Electromagnetic	Photon γ	0	1	∞	$1/137$	$\backsim 10^{-2}$
Strong	Gluon $(\times 8)$ g	0	1	$\backsim 10^{-15}$ m	$\backsim 1$	$\backsim 1$
Weak	$W^{\pm}$ Z^0	80.4 91.2	1 1	$\backsim 10^{-18}$ m	$1/29$	$\backsim 10^{-8}$
Gravity	Graviton?	0	2?	∞	-	$\backsim 10^{-41}$

The Higgs Boson is unique in that it interacts with the other particles with couplings proportional to their masses. It is an excitation of the vacuum Higgs field, responsible for giving mass to particles.

[a] in GeV
[b] Relative strength on the scale of the quarks

Operator	Strong	EM	Weak
Charge Q	✓	✓	✓
Baryon number	✓	✓	✓
Lepton number	✓	✓	✓
Parity $\mathcal{P}$	✓	✓	
Charge conjugation $\mathcal{C}$	✓	✓	
$\mathcal{CP}$	✓	✓	almost
Strangeness	✓	✓	
Charm	✓	✓	
Bottomness	✓	✓	
Isospin	✓		

Table 4.1: Properties conserved in each type of reaction. Blank entries imply that the quantity is not conserved. The combined $\mathcal{CP}$ operation is almost conserved in the weak interaction

4.1.1 Leptons

The class of matter particles that we have not yet met are the *leptons*. These are spin-half fermions that cannot undergo strong interactions as they do not carry any colour charge. Like with the quarks, there are three generations of leptons. The lightest generation contains the electron e^- and its partner neutrino ν_e. The second consists of the muon μ^- and its partner neutrino ν_μ. The muon is negatively charged, with a mass $\backsim$ 200 times that of an electron. The muon lifetime is 2.2 μs after which it decays as

$$\mu^- \longrightarrow e^- + \bar{\nu}_e + \nu_\mu \tag{4.1}$$

which is shown in the first order Feynman diagram figure 4.2 below. Note that the decay is via a weak interaction.

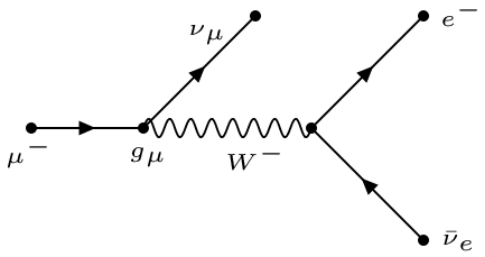

Figure 4.2: The first order Feynman diagram for μ_- decay

The third generation contains the tau τ^- and its neutrino ν_τ. It is once again negatively charged, but is much more massive, $\backsim$ 3500 times that of an electron. As such, it decays very rapidly in 2.9×10^{-13} s. The τ can decay into either a $e^-\bar{\nu}_e$ or $\mu^-\bar{\nu}_\mu$ pair, but due to its large mass, hadronic decays are also possible, such as

$$\tau^- \longrightarrow \begin{cases} \pi^- + \nu_\tau \\ \pi^- + \pi^0 + \nu_\tau \\ \pi^- + \pi^+ + \pi^- + \nu_\tau \\ K^- + \nu_\tau \end{cases}$$

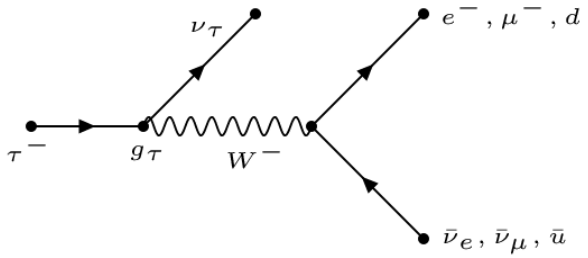

Figure 4.3: The first order Feynman diagram for τ_- decay

An important property of leptons is that of *lepton universality*; each of the families of leptons couples in the same way to the W boson. Furthermore, each of the charged leptons/neutrinos couples to the Z boson in the same way. We can confirm this by looking at the decays of μ^- and τ^- into a $e^-\nu_e$ pair. Using (2.43), we have that $\Gamma \propto Q^5 \propto m_{CM}^5$ for relativistic particles. We thus expect the decay rates of the particles to scale as

$$\frac{\Gamma(\tau^- \to e^- + \bar{\nu}_e + \nu_\tau)}{\Gamma(\mu^- \to e^- + \bar{\nu}_e + \nu_\mu)} = \left(\frac{m_\tau}{m_\mu}\right)^5 \tag{4.2}$$

If lepton universality is to hold, the vertex coupling constants g_μ and g_τ should be equal:

$$\left(\frac{g_\tau}{g_\mu}\right)^2 = \underbrace{\frac{B(\tau^- \to e^- + \bar{\nu}_e + \nu_\tau)}{B(\mu^- \to e^- + \bar{\nu}_e + \nu_\mu)}}_{=0.178} \left[\frac{\Gamma(\tau^-)}{\Gamma(\mu^-)}\right]^{-1} \frac{\tau_\mu}{\tau_\tau} = 0.178 \left(\frac{m_\tau}{m_\mu}\right)^5 \frac{\tau_\mu}{\tau_\tau} \approx 0.999 \tag{4.3}$$

where we have used the fact that $\Gamma = \tau^{-1} \propto g^2 m^5$, as well as known values for the masses and lifetimes of the muon and tau leptons. We see that the coupling constants are of order unity, as expected.

It is useful to define quantum numbers that count the number of leptons. *Lepton flavour numbers* are the number of leptons of each generation less the number of corresponding anti-leptons of that generation:

$$\begin{aligned} L_e &= N(e^-) + N(\nu_e) - N(e^+) - N(\bar{\nu}_e) \\ L_\mu &= N(\mu^-) + N(\nu_\mu) - N(\mu^+) - N(\bar{\nu}_\mu) \\ L_\tau &= N(\tau^-) + N(\nu_\tau) - N(\tau^+) - N(\bar{\nu}_\tau) \end{aligned} \tag{4.4}$$

We cam also define the *total lepton number* $L_\ell = L_e + L_\mu + L_\tau$, which is conserved in all known reactions. The individual lepton flavour numbers are also conserved in most reactions, the notable exception being neutrino oscillations, which we shall discuss in section 4.4.

4.2 The Strong Interaction

Let us revisit the strong interaction. This is mediated by the spin-one, massless particles that are *gluons*. Gluons carry both quark colour and anti-colour, and there are only eight orthogonal gluon states because one of the nine possible colour-anticolour combinations is colourless:

$$\frac{1}{\sqrt{3}}(|r\bar{r}\rangle + |g\bar{g}\rangle + |b\bar{b}\rangle) \tag{4.5}$$

The strong coupling constant $\alpha_S \backsim 1$ is larger than the electromagnetic coupling constant $\alpha_{\text{EM}} = 1/137$, meaning that if both forces are present, the strong interaction tends to dominate any reaction modes (as previously stated). However, the strong force is more than just a stronger version of the electromagnetic interaction. Gluons (unlike photons) can act as sources for their own field. This means that there is a gluon self-interaction force, involving a three-gluon interaction vertex, which leads to new behaviours.

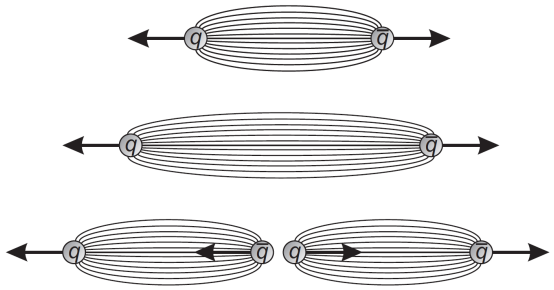

Figure 4.4: A toy model of quark confinement

Consider the pulling apart of a quark-antiquark pair. These are held together by field of virtual gluons, which forms a thin tube between them. As we pull the quarks apart, potential energy is built up in this field, manifesting as the spring-like term in (3.33). Eventually, this energy is large enough that it is energetically favourable for the tube to break up by dragging multiple $q\bar{q}$ pairs out of the vacuum. The resulting hadrons can be observed in relativistic *jets* formed due to the headlight effect. This is the essence of *quark confinement*; we can never observe a free quark, as it will just use part of its kinetic energy to create hadrons out of the vacuum.

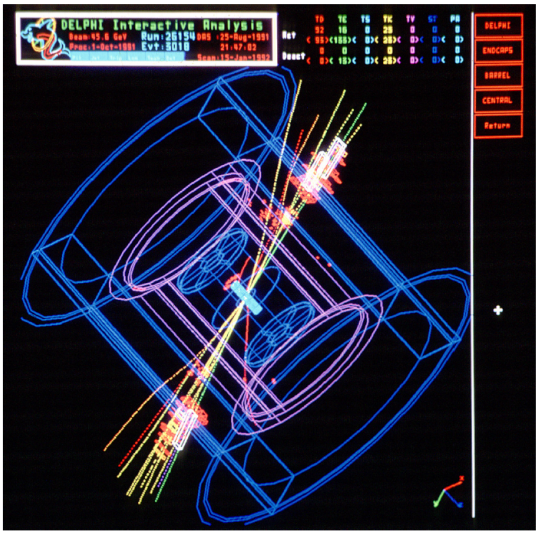

Figure 4.5: A two jet event at an e^+e^- centre of mass energy close to 100 GeV

4.2.1 Deep Inelastic Scattering

Though we cannot isolate individual quarks, we are still able to perform scattering experiments at the quark level, known as *deep inelastic scattering.* For this, we need to use particles that are of sufficiently high energy ($\backsim$ GeV) such that their de-Broglie wavelength is comparable to the size of the proton (for example). This means that they will not scatter from the proton as a whole, instead undergoing scattering events with the individual quarks inside the proton.

These events pull the scattered quark away from the other quarks, which will create a hadron jet in the original direction of the outgoing quark if energies are sufficiently high. The other *spectator quarks* in the proton also form a coloured state, meaning that they must create hadrons in another jet event.

The interaction between the electron and the quark can either be mediated by the weak or electromagnetic forces. If the propagator is a $W^{\pm}$, then the collision is said to include a *weak charged current*, and the flavour of the scattered quark is changed. In the case of the Z^0 or γ, these are known as *weak neutral current* and *weak electromagnetic interaction* respectively, in which the quark flavour is unchanged.

At low values of the momentum transfer Q, the ratio of weak interactions to electromagnetic interactions is very small, where as at high values, it is of order unity. Consider the propagators:

$$G_\gamma = -\frac{1}{\mathsf{Q}^2}, \quad G_W = -\frac{1}{\mathsf{Q}^2 + m^2c^2} \tag{4.6}$$

For low values of Q, $m(W^{\pm}, Z^0)c^2 \gg \mathsf{Q}$ as the $W^{\pm}$ and Z^0 bosons are very massive, meaning that $G_\gamma \gg G_W$. However, as Q becomes very large, we can neglect the rest mass energies of these gauge bosons, such that the ratio of G_γ/G_W tends to unity.

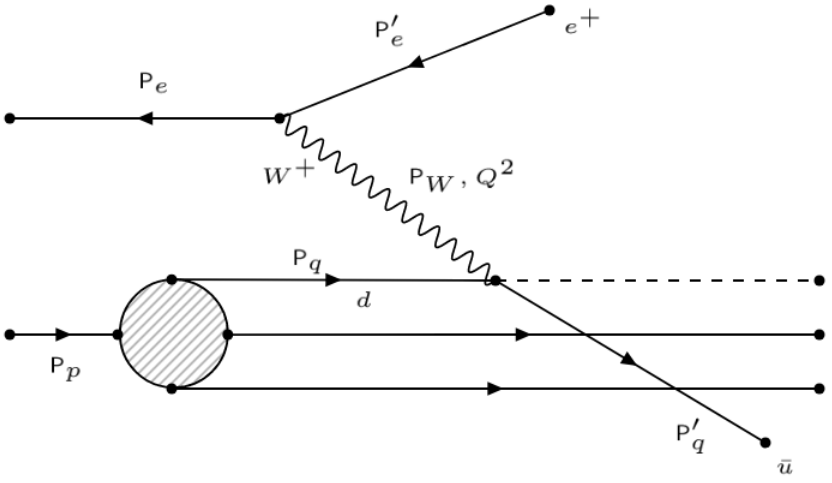

Figure 4.6: A positron-proton scattering event under weak charged current

Let us consider an example of a positron-proton scattering event in the deep-inelastic regime. We define the four-momenta

$$\mathsf{P}_e = (E_e/c, \mathbf{p}_e), \quad \mathsf{P}'_e = (E'_e/c, \mathbf{p}'_e), \quad \mathsf{P}_q = x\mathsf{P}_p \tag{4.7}$$

where we have defined the quark to have some fraction $0 < x < 1$ of the original proton

momentum. Using invariants, we have that

$$-\mathsf{Q}^2 = \frac{(E_e - E'_e)^2}{c^2} - (\mathbf{p}_e - \mathbf{p}'_e)^2 \approx -\frac{2E_e E'_e}{c^2}(1 - \cos\theta) \tag{4.8}$$

where the second expression follows from neglecting the rest mass energy of the positrons, as they are sufficiently relativistic in deep inelastic scattering events. θ is the angle through which the positron is scattered. Thus, the momentum transfer Q is given by

$$\mathsf{Q}^2 = \frac{4E_e E'_e}{c^2}\sin^2\left(\frac{\theta}{2}\right) \tag{4.9}$$

The centre of mass energy is given by

$$s = (\mathsf{P}_e + \mathsf{P}_q)^2 c^2, \quad E_{CM} = \sqrt{s} \tag{4.10}$$

for the positron-quark system. Then,

$$s = (\mathsf{P}_e^2 + \mathsf{P}_q^2 + 2\mathsf{P}_e \cdot \mathsf{P}_q)c^2 = (m_e^2 c^2 + x^2 m_p^2 c^2 + 2x\mathsf{P}_e \cdot \mathsf{P}_p)c^2 \tag{4.11}$$

We then assume that the particles are approximately massless at these relativistic energies, meaning that we can neglect the rest mass energies, and use

$$|\mathbf{p}_e| \approx \frac{E_e}{c}, \quad |\mathbf{p}_p| \approx \frac{E_p}{c}, \quad \mathbf{p}_e \cdot \mathbf{p}_p = -|\mathbf{p}_e||\mathbf{p}_p| \tag{4.12}$$

where we have assumed that the positron and proton collide head on. With these assumptions, we arrive at the final result of

$$\boxed{s = 4xE_e E_p, \quad E_{CM} = \sqrt{s}} \tag{4.13}$$

Thus, the centre of mass energy available for the production of hadrons is proportional to the square root of the geometric mean of the energies of the positron and quark.

Detectors

How do we detect the particles produced in the jets associated with deep inelastic scattering? The momentum of the antielectron can be determined using the inner part of the detector (the *tracker*) that tracks the trajectory of charged particles, and measures their momenta as they bend in an externally applied field. The direction of curvature of the track (relative to the magnetic field) allows the sign of the charge to be deduced, while the radius of curvature R permits the calculation of the perpendicular component of the momentum from

$$|\mathbf{p}_\perp| = qBR \tag{4.14}$$

The *calorimeter* lies outside the tracker, and is designed to stop particles and convert their energies into an electrical signal. This allows the other components of the momentum to be determined.

Neutrinos (where produced) cannot be directly detected in such scattering experiments as they are so weakly interacting. However, we can determine the perpendicular component of their momentum from momentum conservation in the perpendicular plane.

4.3 The Weak Interaction

The weak interaction is mediated by three spin-one bosons: the charged $W^{\pm}$ (antiparticles of one another), and the neutral Z^0 (its own antiparticle). The weak force is very short ranged as a result of their large masses:

$$m_W = 80.3\ \text{GeV}/c^2, \quad m_Z = 91.2\ \text{GeV}/c^2 \tag{4.15}$$

from which we approximate their range $\hbar c/mc^2$ is about 2×10^{-3} fm, which is about 1000 times smaller that the size of a proton. As stated previously, the coupling of leptons to the W boson is universal, with vertex factor g_W. This means that decays of $W^{\pm}$ into any of the three lepton generations is equally likely (as the density of states is roughly the same in these highly relativistic decays).

4.3.1 Quark Mixing

The weak interaction is the only type of interaction that can change quark flavour, which only occurs in interactions mediated by the $W^{\pm}$ bosons.

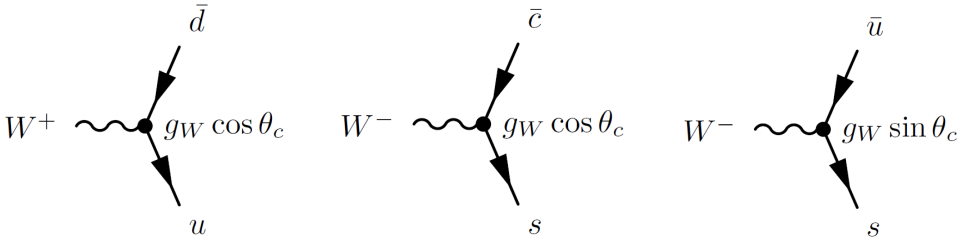

Figure 4.7: The coupling of the $W^{\pm}$ bosons to quarks (a) $u\bar{d}$ (b) $\bar{c}s$ (c) $\bar{u}s$ (suppressed)

A vertex involving a $W^{\pm}$ and two quarks must include an upper $Q = 2/3$ and lower $Q = -1/3$ quark, in order to conserve charge. The vertices that include two quarks of the same generation dominate, while those involving transitions between those of different generations are suppressed. To see why this is, let us consider each of the 'lower' quarks to have their our weak interaction eigenstates $|d'\rangle$, $|s'\rangle$ and $|b'\rangle$, each of which is a superposition of the mass eigenstates $|d\rangle$, $|s\rangle$ and $|b\rangle$ (the observable eigenstates). The $|u\rangle$, $|c\rangle$ and $|t\rangle$ couple to the $|d'\rangle$, $|s'\rangle$ and $|b'\rangle$ states respectively.

Let us consider the simple case of just the down and strange quarks. In the interaction basis, the couplings of the $W^{\pm}$ are diagonal, so the (W, u, d') and the (W, c, s') couplings take the same value g_W, where as the couplings (W, u, s') and (W, c, d') are each zero. The flavour eigenstates $\{|d'\rangle, |s'\rangle\}$ in the primed basis must differ from the mass eigenstates $\{|d\rangle, |s\rangle\}$ in the unprimed basis, as we do indeed observe cross-generational quark mixing. This is done by a rotation:

$$\boxed{\begin{pmatrix} |d'\rangle \\ |s'\rangle \end{pmatrix} = V_c \begin{pmatrix} |d\rangle \\ |s\rangle \end{pmatrix}, \quad V_c = \begin{pmatrix} \cos\theta_c & -\sin\theta_c \\ \sin\theta_c & \cos\theta_c \end{pmatrix}} \tag{4.16}$$

V_c is the 2×2 *Cabibbo rotation matrix* (or *CKM* matrix), while $\theta_c \approx 13°$ is the *Cabibbo rotation angle*. As this rotation angle is small, this means that interactions that change generation are heavily suppressed, while interactions that do not change generation are not. If we include the full basis, this becomes a 3×3 matrix, with couplings between generations I and III being suppressed.

4.3.2 Production and Decay of $W^{\pm}$ and Z^0

The weak bosons can be produced in $p\bar{p}$ collisions where a quark from the proton and an antiquark from the anti proton annihilate. For this to occur, the centre of mass energy of the system has to be in the region of ≈ 540 GeV. To produce a Z^0 boson, the quarks must be of the same flavour - either $u\bar{u}$ or $d\bar{d}$. To produce $W^{\pm}$, the combinations $u\bar{d}$ and $\bar{u}d$ are required respectively. Neither the $W^{\pm}$ nor Z^0 are massive enough to decay into a top quark as it is too massive.

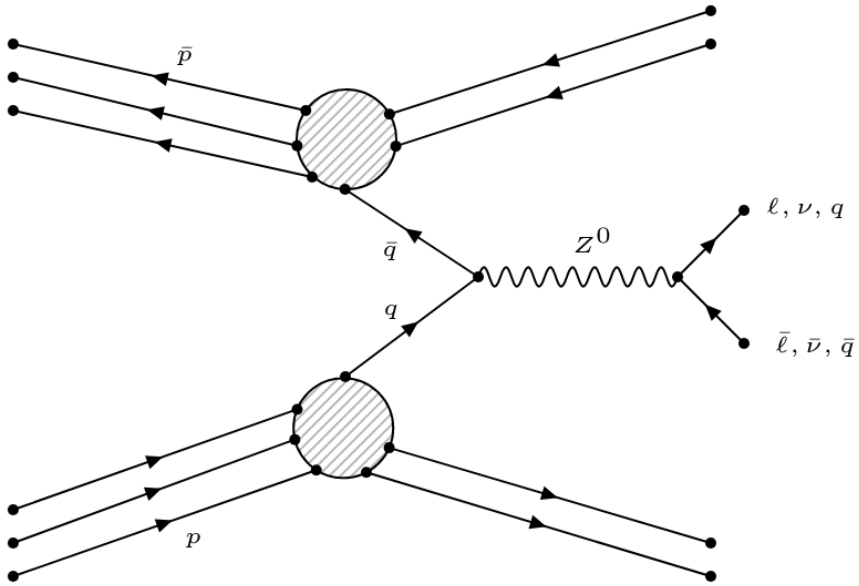

Figure 4.8: A Feynman diagram showing the production and decay of a Z^0 boson

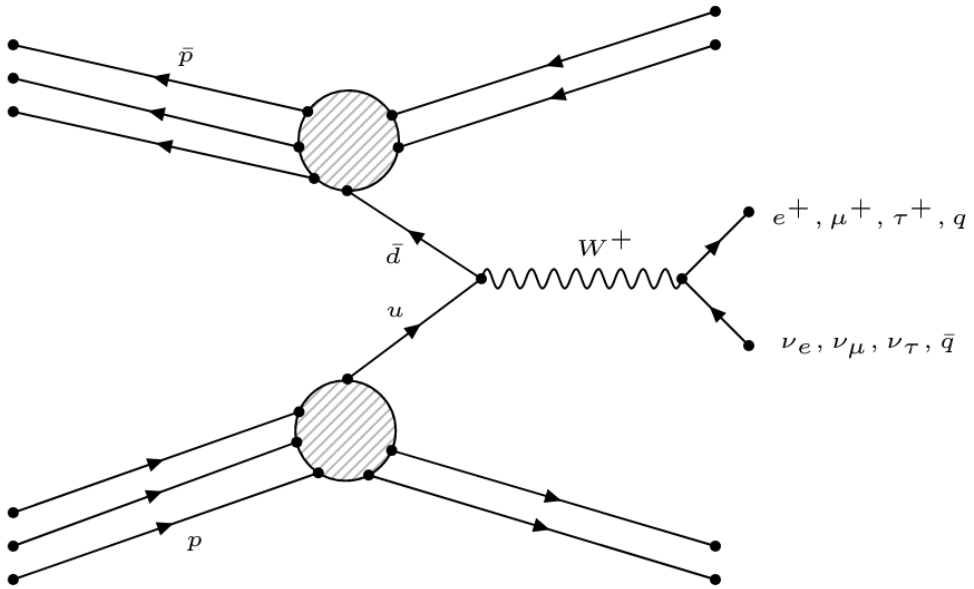

Figure 4.9: A Feynman diagram showing the production and decay of a W^+ boson

Consider the production of the Z^0. If the quark carries momentum fraction x_1 of the proton and the antiquark carries momentum fraction x_2 of the antiproton, then to produce a Z^0 close to its mass shell - where the cross section is at its maximum - we require that:

$$m_Z^2 c^2 = -(\mathsf{P}_q + \mathsf{P}_{\bar{q}})^2 \approx -2x_1 x_2 \mathsf{P}_p \cdot \mathsf{P}_{\bar{p}} = x_1 x_2 \times E_{CM}(p\bar{p}) \tag{4.17}$$

The Z^0 boson is able to decay into any neutral combination of hadrons and leptons. This leads to the possible final states of:

Decay Path	Relative Decay Rate
$q\bar{q}$	3×5
e^+e^-	1
$\mu^+\mu^-$	1
$\tau^+\tau^-$	1
$\nu_e\bar{\nu}_e$	1
$\nu_\mu\bar{\nu}_\mu$	1
$\nu_\tau\bar{\nu}_\tau$	1

The extra factor of three in the $q\bar{q}$ decay path comes from the three different available colour combinations. This means that we have the branching ratios

$$\frac{\sum \Gamma_{q\bar{q}}}{\Gamma} = \frac{5}{7}, \quad \frac{\sum \Gamma_{\ell\bar{\ell}}}{\Gamma} = \frac{1}{7}, \quad \Gamma_{\nu\bar{\nu}} = \frac{1}{21} \tag{4.18}$$

The total partial width for the decay of the Z^0 boson is given by

$$\Gamma = \sum \Gamma_{q\bar{q}} + \sum \Gamma_{\ell\bar{\ell}} + \Gamma_{\text{invis}} \tag{4.19}$$

The invisible width corresponds to the rate of decay to neutrinos (invisible as the neutrinos cannot be detected in these scattering experiments) is given by the simply product of the partial width for a given neutrino pair $\Gamma_{\nu\bar{\nu}}$ times the number of pairs:

$$\Gamma_{\text{invis}} = N_\nu \times \Gamma_{\nu\bar{\nu}} \tag{4.20}$$

The total width Γ can be measured experimentally, while $\Gamma_{\nu\bar{\nu}}$ can be calculate from the related process of neutral-current scattering of neutrinos. This allowed the CERN group to determine

$$N_\nu = 2.984 \pm 0.008 \tag{4.21}$$

which is consistent with the three-generational model for neutrinos.

The W^+ can decay into the following possible final states:

Decay Path	Relative Decay Rate
$u\bar{d}$	3×1
$c\bar{s}$	3×1
$e^+\nu_e$	1
$\mu^+\nu_\mu$	1
$\tau^+\nu_\tau$	1

In principle, bottom quark decays are also possible, but these are suppressed through the CKM matrix coupling. It is clear from the above that the hadronic decays of W^+ have a higher branching ratio that leptonic decays, meaning that we would expect to have discovered the W^+ through the former decay mode. However, the hadronic jets produced by the W^+ boson decay are not uniquely distinguishable from all other processes that create hadronic jets and are not mediated by the W^+ boson. For example, we could have $q\bar{q}$ scattering, which are strong decays, obscuring the observation of W^+ decay into hadrons. This is why the W^+ was discovered in leptonic decay modes.

4.4 Neutrino Oscillations

As stated in section 4.1.1, individual lepton flavours are not always conserved. This means that if flavour eigenstates are not eigenstates of the Hamiltonian of the system, then lepton flavour is not a conserved quantity, and the amplitude to find the neutrino in a particular flavour eigenstate will be a time-dependent quantity.

Let us consider a simplified neutrino system, that we can characterise by the energy (mass) eigenstates $|\nu_1\rangle$ and $|\nu_2\rangle$, with the latter being more energetic than the former. The flavour eigenstates $|\nu_e\rangle$ and $|\nu_\mu\rangle$ are mixtures of the energy eigenstates

$$|\nu_e\rangle = \cos\theta\,|\nu_1\rangle + \sin\theta\,|\nu_2\rangle \tag{4.22}$$

$$|\nu_\mu\rangle = -\sin\theta\,|\nu_1\rangle + \cos\theta\,|\nu_2\rangle \tag{4.23}$$

where θ is the mixing angle. Assume that the neutrino starts off as an electron-type neutrino at some initial position $\mathbf{x} = 0$. At later times, the neutrinos state is given by

$$|\psi(L,T)\rangle = \cos\theta e^{-i\phi_1}\,|\nu_1\rangle + \sin\theta e^{-i\phi_2}\,|\nu_2\rangle\,, \quad \phi_i = (E_i T - |\mathbf{p}_i|L)/\hbar \tag{4.24}$$

where we have reduced to a single spatial dimension for the propagating wave (without loss of generality), and L and T are the values of position and time at which we measure the neutrino after its oscillation. The probability of flavour change is thus

$$P(\nu_e \to \nu_\mu) = |\langle\nu_\mu|\psi(L,T)\rangle|^2 = \sin^2(2\theta)\sin^2\left(\frac{\phi_1 - \phi_2}{2}\right) \tag{4.25}$$

This phase difference can be written as

$$\hbar\Delta\phi \equiv \hbar(\phi_1 - \phi_2) = (E_1 - E_2)\left(T - \frac{E_1 + E_2}{|\mathbf{p}_1| + |\mathbf{p}_2|}L\right) + \frac{m_1^2c^2 - m_2^2c^2}{|\mathbf{p}_1| + |\mathbf{p}_2|}L \tag{4.26}$$

We now demand that energy must be conserved, such that $E_1 = E_2$, such that

$$\Delta\phi = \frac{m_1^2c^2 - m_2^2c^2}{\hbar\left(|\mathbf{p}_1| + |\mathbf{p}_2|\right)}L \approx \frac{\Delta m^2 c^3 L}{4\hbar E} \tag{4.27}$$

where we have assumed that the neutrinos have negligible rest mass energy in comparison to their momentum, and $\Delta m^2 = m_1^2 - m_2^2$. We thus arrive at the final result of

$$\boxed{P(\nu_e \to \nu_\mu) = \sin^2(2\theta)\sin^2\left(\frac{\Delta m^2 c^3 L}{4\hbar E}\right)} \tag{4.28}$$

In more convenient units, the arguments of the oscillation can be written

$$\frac{\Delta m^2 c^3 L}{4\hbar E} = 1.3\frac{\Delta m^2 c^2}{\mathrm{eV}^2}\frac{L}{\mathrm{km}}\frac{\mathrm{GeV}}{E} \tag{4.29}$$

As the mass differences (as well as the masses themselves) are quite small, this oscillation will happen over the distance of many kilometres. These long distances come from a combination of the near-degeneracy of the masses, and the neutrinos' large Lorentz factors ($\backsim 10^{12}$), meaning that they are subject to a very large time dilation. Neutrinos detected in experiments are usually produced in solar *pp* fusion reactions (ν_e), or in pion and muon decays (ν_e, ν_μ) in the atmosphere. Due to their weak interaction with matter, neutrinos are usually detected using vast quantities of water in order to increase the probability of interaction, and this detection.